

Vertex nomination between graphs via spectral embedding and quadratic programming

Runbing Zheng

Department of Statistics, North Carolina State University

Vince Lyzinski*

Department of Mathematics, University of Maryland

Carey E. Priebe

Department of Applied Mathematics and Statistics, Johns Hopkins University

Minh Tang

Department of Statistics, North Carolina State University

March 29, 2022

Abstract

Given a network and a subset of interesting vertices whose identities are *only partially* known, the vertex nomination problem seeks to rank the remaining vertices in such a way that the interesting vertices are ranked at the top of the list. An important variant of this problem is vertex nomination in the multiple graphs setting. Given two graphs G_1, G_2 with common vertices and a vertex of interest $x \in G_1$, we wish to rank the vertices of G_2 such that the vertices most similar to x are ranked at the top of the list. The current paper addresses this problem and proposes a method that first applies adjacency spectral graph embedding to embed the graphs into a common Euclidean space, and then solves a penalized linear assignment problem to obtain the nomination lists. Since the spectral embedding of the graphs are only unique up to orthogonal transformations, we present two approaches to eliminate this potential non-identifiability. One approach is based on orthogonal Procrustes and is applicable when there are enough vertices with known correspondence between the two graphs. Another approach uses adaptive point set registration and is applicable

*VL research is sponsored by the Air Force Research Laboratory and DARPA under agreement number FA8750-20-2-1001. The U.S. Government is authorized to reproduce and distribute reprints for Governmental purposes notwithstanding any copyright notation thereon. The views and conclusions contained herein are those of the authors and should not be interpreted as necessarily representing the official policies or endorsements, either expressed or implied, of the Air Force Research Laboratory and DARPA or the U.S. Government.

when there are few or no vertices with known correspondence. We show that our nomination scheme leads to accurate nomination under a generative model for pairs of random graphs that are approximately low-rank and possibly with pairwise edge correlations. We illustrate our algorithm’s performance through simulation studies on synthetic data as well as analysis of a high-school friendship network and analysis of transition rates between web pages on the Bing search engine.

Keywords: vertex nomination, correlated graphs, generalized random dot product graphs, point set registration

1 Introduction

Graphs are widely used to model data in various fields wherein vertices represent entities or objects of interest and the edges represent pairwise relationships between the vertices. For example, in social network graphs the vertices represent individuals with the edges showing the communication between these individuals. Another example is citation network where the vertices represent articles and the (directed) edges represent citations between the articles. Finally, in many neuroscience applications, the vertices represent brain regions of interest and the edges summarize the inter-connectivity between these regions. Due to the prevalence of network data, there has been a great deal of research done recently in statistical inference on graphs, including, but not limited to, estimation of graph parameters, (Lloyd et al., 2012; Xu, 2017), one-sample and multi-sample hypothesis testing (Moreno and Neville, 2013; Tang et al., 2017), graph clustering and classification (Kudo et al., 2005; Schaeffer, 2007; Yin et al., 2017; Zhang et al., 2018), and vertex nomination (Fishkind et al., 2015; Yoder et al., 2020).

Vertex nomination is the graph analog of recommender systems for general tabular data. The simplest and most widely studied variant of this problem is in the single graph setting wherein, given a network and a subset of interesting vertices whose identities are partially known, the task is to identify, using the known interesting vertices, the remaining vertices of interest. The number of interesting vertices is, in general, much smaller than the total number of vertices in the graphs, and vertex nomination algorithms usually seek to output a list of candidate vertices (that are deemed interesting) with the aim that the remaining true but unknown vertices of interest are concentrated near the top of the list.

The vertex nomination problem in the single graph setting appears, at first blush, to be similar to the more widely studied community detection problem (Duch and Arenas, 2005; Fortunato, 2010; Newman, 2006); however, there are important conceptual and practical differences between the two. More specifically, community detection is concerned with clustering or partitioning *all* the vertices of a network into communities or clusters; a cluster is, roughly speaking, a group of vertices exhibiting a different connectivity pattern within the cluster as compared to the connectivity between clusters. In contrast, as we alluded to earlier, vertex nomination is only concerned with identifying a small subset of vertices of interest, and furthermore, these vertices of interest might not form a cluster in the usual sense, e.g., their intraconnectivity does not need to be qualitatively different from their connectivity to other "non-interesting" vertices. Due to this reason, vertex nomination is also not the same as local graph clustering (Spielman and Teng, 2013; Yin et al., 2017) as local graph clustering is concerned with clustering the vertices around the neighbourhood of a given seed vertex; the unknown vertices of interest might or might not be included in that neighbourhood.

Before continuing with our exposition we emphasize that, similar to recommender systems for tabular data or community detection in networks, vertex nomination is intrinsically an unsupervised learning problem. It is universally accepted that these type of problems generally do not have clearly defined solutions. For example, given a collection of data points in \mathbb{R}^d , there can be numerous different ways to group these data points into clusters and furthermore all of these clusterings can be valid, and the preference for one clustering over another clustering depends on the setting and/or objective of the data analysis at hand. Analogously, given a graph G , what characterizes a vertex v or a collection of vertices S in G as being interesting is in general not well-defined and could vary between applications and/or between users. Therefore, to present a relevant notion of "interestingness", it is usually assumed that there exists a generative process underlying the observed graph(s); the process itself could be latent or partially observed. This is similar to the use of stochastic block models or its variants in the context of community detection, the use of the Bradley-Terry model in ranking problems, and the assumption of low-rank fac-

tor models in recommender systems. Furthermore, even when we assume that the latent generative model belongs to a collection of models denoted by \mathcal{M} , if \mathcal{M} is not sufficiently restricted then there does not exist a vertex nomination algorithm that is well-behaved for all models in \mathcal{M} , i.e., for any algorithm \mathcal{A} there exists a model $M_0 \in \mathcal{M}$ such that the nomination accuracy of \mathcal{A} when given data generated from M_0 is no better than random guessing; see [Lyzinski et al. \(2019\)](#) for a more precise formulation and statement of this result. In light of the above discussion, in this paper we shall present our methodology in the context of a generative model for which there are latent but unobserved features associated with the vertices and, from these latent features, we can define an appropriate notion of “interestingness”. Similarly, our real data analysis examples are motivated by datasets where there are one-to-one correspondence between (a subset of) the vertices.

Typical applications of vertex nomination include predicting group membership in social networks ([Coppersmith and Priebe, 2012](#)), searching and indexing in databases ([Levin, 2017](#)), and identifying specific type of neurons (e.g., motor neurons) in neuroscience ([Fishkind et al., 2015](#)). A sizable number of techniques have been developed for vertex nomination in the single graph setting, including methods based on likelihood maximization, Bayesian MCMC, and spectral decomposition of the adjacency matrices, see [Coppersmith and Priebe \(2012\)](#); [Fishkind et al. \(2015\)](#); [Lee and Priebe \(2012\)](#); [Lyzinski et al. \(2016\)](#); [Sun et al. \(2012\)](#); [Yoder et al. \(2020\)](#) and the references therein. Among these diverse techniques, the spectral decomposition approach is one of the most practical as it is computationally efficient and can be scaled to handle reasonably large and sparse networks.

The current paper focuses on another important, albeit much less studied, variant of the vertex nomination problem, namely vertex nomination across graphs. More specifically, given two networks G_1 and G_2 and a vertex of interest x in the network G_1 , our task is to find the corresponding vertex of x in G_2 (if it exists). We emphasize that G_1 and G_2 need not have the same number of vertices and that the correspondence between the vertices of G_1 and G_2 is largely unknown. The following is a concrete practical example of the above problem. Consider the pair of high school friendship networks ([Patsolic et al., 2017](#)). The

first social network G_1 , having 156 vertices, represents a Facebook network, in which two vertices are adjacent if the pair of individuals are friends on Facebook. The second social network G_2 with 134 vertices, is created based on the result of survey, and two vertices are adjacent if the students report they are friends. There are 82 students appearing in both social network G_1 and G_2 . Given a student of interest in G_1 , our goal is to identify the corresponding student in G_2 . We may know the corresponding relationship of some other shared students, and the information can help us to nominate the student of interest in G_2 . This is a typical example, and similar examples could be constructed including (1) identifying which user in Instagram corresponding to some specific user in Facebook, (2) identifying topics of interest across graphical knowledge bases (Sun and Priebe, 2013) and (3) identifying structural signal across connectomes (Sussman et al., 2020).

Two algorithms were recently proposed for this multi-graph vertex nomination problem. The authors of Agterberg et al. (2020) proposed an algorithm based on spectral graph embedding wherein (1) the graphs are spectrally embedded into Euclidean space, (2) the embedded points are aligned via orthogonal Procrustes transformation, (3) the embedded points are simultaneously clustered via Gaussian mixture modeling (Fraley and Raftery, 1998), and (4) output the candidate vertices using the resulting clustering. In contrast, the authors of Patsolic et al. (2017) proposed an algorithm based on seeded graph matching (Lyzinski et al., 2014) wherein they graph match induced subgraphs generated around neighbourhoods of the vertices with known correspondence in each network.

The proposed algorithm in this paper also uses spectral graph embedding. It is noted, empirically, that spectral graph embedding approaches are much faster and more scalable, computationally, as compared to graph matching approaches. Our approach is similar to Agterberg et al. (2020) in that we also spectrally embed the graphs into a common Euclidean space. However, in contrast to the Gaussian mixture modeling of Agterberg et al. (2020), our nomination lists are based on solving a penalized linear assignment problem, and are thus not dependent on tuning parameters such as the number of clusters and the shape/orientation of these clusters, both of which are hard to tune and could have significant impacts on the ordering in the nomination lists. Indeed, if the embedding dimension d is

moderately large, a Gaussian mixture model with arbitrary covariance matrices requires estimation of $O(Kd^2)$ parameters where K is the maximum number of Gaussian component.

We also prove consistency results about our scheme when the number of vertices goes to infinity under mild assumptions for a wide class of popular random graph models. Furthermore, for a class of random graph model where the edges of the two graphs are pairwise correlated, we analyze how the magnitude of this correlation influences the consistency.

2 Methodology

We first introduce some notations. Let the two graphs be denoted as $G_1 = (V_1, E_1)$ and $G_2 = (V_2, E_2)$ where V_1 and V_2 are the vertices sets and E_1 and E_2 are the edges sets. We shall assume that our graphs are *undirected*. We also partition the vertices sets V_1 and V_2 as $V_1 = U_1 \cup J_1$ and $V_2 = U_2 \cup J_2$ where U_1 and U_2 denote the sets of *shared* vertices between G_1 and G_2 . We emphasize that the correspondence between the vertices in U_1 and U_2 are only partially known, i.e, we further partition U_1 and U_2 as $U_1 = \{x\} \cup S_1 \cup W_1$ and $U_2 = \{\sigma(x)\} \cup S_2 \cup W_2$ where x denote the *known* vertex of interest in G_1 ; $\sigma : U_1 \rightarrow U_2$ is a bijection such that for any $v \in U_1$, $\sigma(v)$ is its corresponding vertex in U_2 ; S_1 and S_2 are the seed sets with $|S_1| = |S_2| = K$, where we already know the corresponding relationship, i.e., we know the bijection $\sigma|_{S_1} : S_1 \rightarrow S_2$; and W_1 and W_2 are the remaining vertices of interest. We shall assume that the mapping σ from W_1 to W_2 is unknown, and furthermore, while the recovery of this correspondence between W_1 and W_2 is important, it is also potentially less pressing than the recovery of $\sigma(x)$. In summary, we only know the correspondence between S_1 and S_2 , and given the known vertex of interest x , we are interested in finding its *unknown* correspondence $\sigma(x) \in V_2 \setminus S_2$. Our goal is thus to seek a nomination list of the vertices in $V_2 \setminus S_2$, ranked according to our confidence in how similar they are to x .

The following example can help to understand how the partitioning of the vertices in each graph arise. We consider the high school friendship network dataset containing two observed graphs. The first graph G_1 is extracted from the Facebook social network and the second graph G_2 is created based on a survey of the students' friendship. These two networks share some students in common. For the first social network G_1 , we partition the

students set V_1 as the union of the set U_1 of shared students and the set J_1 of remaining students. Similarly, we also have the partition $V_2 = U_2 \cup J_2$ for G_2 . There is a bijection between the shared students of the two social networks, but we only observe this bijection for a subset of the vertices; we denote these sets as $S_1 \subset U_1$ and $S_2 \subset U_2$. We have interest in the unknown corresponding relationship. For a specific student of interest $x \in U_1 \setminus S_1$, our goal is to find which vertex $\sigma(x)$ in the second graph corresponds to the same student. We then use $W_1 = U_1 \setminus \{x\} \setminus S_1$ and $W_2 = U_2 \setminus \{\sigma(x)\} \setminus S_2$ to denote the remaining students. More details for the high school friendship network data can be found in Section 4.2.1.

We now describe our algorithm for finding $\sigma(x)$. Our algorithm proceeds in three main steps. In the first step we spectrally embed each graph into some d -dimensional Euclidean space. We next aligned these embeddings either via solving an orthogonal Procrustes problem in the case when K , the number of seeds vertices, is at least as large as the embedding dimension d , or via solving a point set registration problem. Finally we solve a quadratic program, using the pairwise distances between the embedded points, to map each vertex $v \in V_1 \setminus S_1$ to some *ordered subset* $\ell(v) \subset V_2 \setminus S_2$; $\ell(v)$ serves as the *nomination list* of the vertices in $V_2 \setminus S_2$ most similar to v . We now describe these steps in detail.

2.1 Adjacency spectral embedding

We spectrally embed the graphs by truncating their eigenvalue decomposition. More specifically, given an $n \times n$ adjacency matrix \mathbf{A} of a graph and a positive integer d for the embedding dimension, we compute

$$\mathbf{A} = \sum_{i=1}^n \lambda_i u_i u_i^\top,$$

where $|\lambda_1| \geq |\lambda_2| \geq \dots$ are the eigenvalues and u_1, u_2, \dots, u_n are the corresponding eigenvectors. The adjacency spectral embedding of \mathbf{A} (into \mathbb{R}^d) is then the $n \times d$ matrix

$$\hat{\mathbf{X}} = [|\lambda_1|^{1/2} u_1, |\lambda_2|^{1/2} u_2, \dots, |\lambda_d|^{1/2} u_d].$$

The rows of $\hat{\mathbf{X}}$ represent the (low-dimensional) embedding of the vertices of \mathbf{A} into \mathbb{R}^d .

In practice, we can choose d by looking at the eigenvalues of the adjacency matrix. A ubiquitous and principled method is to examine the so-called scree plot and look for

“elbow” or “knees” defining the cut-off between the top (signal) d dimensions and the noise dimensions. [Zhu and Ghodsi \(2006\)](#) provides an automatic dimensionality selection procedure to look for the “elbow” by maximizing a profile likelihood function. [Han et al. \(2019\)](#) suggests another universal approach to rank inference via residual subsampling for estimating rank d . We can also determine d by eigenvalue ratio test ([Ahn and Horenstein, 2013](#)) or by empirical distribution of eigenvalues ([Onatski, 2010](#)).

2.2 Orthogonal Procrustes and point set registration

We applied adjacency spectral embedding to the graphs G_1 and G_2 , thereby obtaining the $n \times d$ matrices $\hat{\mathbf{X}}_1$ and $\hat{\mathbf{X}}_2$, respectively. As the rows of $\hat{\mathbf{X}}_1$ and $\hat{\mathbf{X}}_2$ represent the low-dimensional embeddings of the vertices in G_1 and G_2 , we should expect that, for similar vertices, these rows are close in ℓ_2 distance. This is, however, not necessarily the case as the embeddings $\hat{\mathbf{X}}_1$ and $\hat{\mathbf{X}}_2$ are not unique, i.e., $\hat{\mathbf{X}}_1$ and $\hat{\mathbf{X}}_2$ are only defined up to some orthogonal transformations as the eigendecomposition of \mathbf{A}_1 is not, in general, unique. We thus need to align $\hat{\mathbf{X}}_1, \hat{\mathbf{X}}_2$ by an orthogonal transformation \mathbf{W} to eliminate this potential non-identifiability. We describe two methods for finding $\hat{\mathbf{W}}$. The first method is applicable when K , the number of seed vertices, is larger than or equal to d , the embedding dimension; the second method, which is more general but possibly less accurate, is applicable for $K < d$, including the important case of $K = 0$.

2.2.1 Orthogonal Procrustes (when $K \geq d$)

When the number of seed vertices is greater than or equal to the embedding dimension, we find the orthogonal transformation $\hat{\mathbf{W}}$ by solving the orthogonal Procrustes problem ([Schönemann, 1966](#)) to align the seeded vertices across graphs, i.e.,

$$\hat{\mathbf{W}} = \arg \min_{\mathbf{W} \in \mathbb{O}_d} \|(\hat{\mathbf{X}}_1)_{S_1} \mathbf{W} - (\hat{\mathbf{X}}_2)_{S_2}\|_F,$$

where \mathbb{O}_d is the set of all $d \times d$ orthogonal matrices and $(\hat{\mathbf{X}}_1)_{S_1}$ is a $|S_1| \times d$ matrix whose rows are the rows of $\hat{\mathbf{X}}_1$ indexed by the seed set S_1 . With $S_2 = \{\sigma(v) : v \in S_1\}$, $(\hat{\mathbf{X}}_2)_{S_2}$ is defined similarly, so that the i th row of $(\hat{\mathbf{X}}_1)_{S_1}$ corresponds to the i th row of $(\hat{\mathbf{X}}_2)_{S_2}$. The

minimizer $\hat{\mathbf{W}}$ has an explicit solution as $\hat{\mathbf{W}} = \mathbf{U}\mathbf{V}^\top$ where $\mathbf{U}\mathbf{D}\mathbf{V}^\top$ is the singular value decomposition of the $d \times d$ matrix $(\hat{\mathbf{X}}_2)_{S_2}^\top (\hat{\mathbf{X}}_1)_{S_1}$. After finding $\hat{\mathbf{W}}$ we set $\tilde{\mathbf{X}}_1 = \hat{\mathbf{X}}_1 \hat{\mathbf{W}}$.

2.2.2 Adaptive rigid point set registration (when $K < d$)

Even when we do not have enough seed vertices or even no seed set ($K = 0$), as long as we have a reasonable number of vertices that are shared between the two graphs, we can apply the coherent point drift algorithm in [Myronenko and Song \(2010\)](#) to align $\hat{\mathbf{X}}_1$ and $\hat{\mathbf{X}}_2$. The algorithm in [Myronenko and Song \(2010\)](#) finds an affine transformation to best align the centroids of the clusters of $\hat{\mathbf{X}}_1$ to the centroids of the clusters of $\hat{\mathbf{X}}_2$. More specifically, given a $n \times d$ matrix $\hat{\mathbf{X}}_1$ and $m \times d$ matrix $\hat{\mathbf{X}}_2$, we find $s \in \mathbb{R}$, $t \in \mathbb{R}^d$ and $\mathbf{W} \in \mathbb{O}_d$ that minimize the following objective function

$$Q(\mathbf{W}, \mathbf{t}, s, \sigma^2) = \frac{1}{2\sigma^2} \sum_{i=1}^n \sum_{j=1}^m P(i | (\hat{\mathbf{X}}_2)_j) \|(\hat{\mathbf{X}}_2)_j - s\mathbf{W}^\top (\hat{\mathbf{X}}_1)_i - \mathbf{t}\|^2 + \frac{N_{\mathbf{P}} d}{2} \log \sigma^2,$$

where $(\hat{\mathbf{X}}_1)_i$ represents the i th row of $\hat{\mathbf{X}}_1$, i.e., the i th vertex's embedding of G_1 ; $(\hat{\mathbf{X}}_2)_j$ is defined similarly. Here $N_{\mathbf{P}} = \sum_{i=1}^n \sum_{j=1}^m P(i | (\hat{\mathbf{X}}_2)_j)$ is a normalizing constant, with $P(i | (\hat{\mathbf{X}}_2)_j)$ the correspondence probability between two vertices' embeddings $(\hat{\mathbf{X}}_1)_i$ and $(\hat{\mathbf{X}}_2)_j$, defined as the posterior probability of the centroid given the vertex's embedding $(\hat{\mathbf{X}}_2)_j$, i.e.,

$$P(i | (\hat{\mathbf{X}}_2)_j) = \frac{\exp\left(-\frac{1}{2} \|((\hat{\mathbf{X}}_2)_j - s\mathbf{W}^\top (\hat{\mathbf{X}}_1)_i - \mathbf{t})/\sigma\|^2\right)}{c + \sum_{k=1}^n \exp\left(-\frac{1}{2} \|((\hat{\mathbf{X}}_2)_j - s\mathbf{W}^\top (\hat{\mathbf{X}}_1)_k - \mathbf{t})/\sigma\|^2\right)},$$

for some constant c (where c is a function of the model parameters defined above; see [Myronenko and Song \(2010\)](#)). The minimization of Q is done via an EM-algorithm. For more details, please refer to [Myronenko and Song \(2010\)](#).

The resulting minimizer $(\hat{s}, \hat{\mathbf{t}}, \hat{\mathbf{W}})$ yield an affine transformation \mathcal{T} of $\hat{\mathbf{X}}_1$ via $\mathcal{T}((\hat{\mathbf{X}}_1)_i) = s\hat{\mathbf{W}}^\top (\hat{\mathbf{X}}_1)_i + \hat{\mathbf{t}}$. We note, however, that in the context of our current work, the alignment of $\hat{\mathbf{X}}_1$ and $\hat{\mathbf{X}}_2$ does not require the scaling s and the translation t . We thus make a few minor adjustments to the EM algorithm in [Myronenko and Song \(2010\)](#). In particular, 1) we always set $s = 1$ and $\mathbf{t} = \mathbf{0}$; 2) we iteratively update \mathbf{W} via $\mathbf{W}^\top = \mathbf{U}\mathbf{V}^\top$ instead of

$\mathbf{W}^\top = \mathbf{UCV}^T$; 3) we initialize \mathbf{W} as a diagonal matrix with 1 or -1 diagonal elements so that the initial error in the EM approach $\sigma^2 = \frac{1}{dnm} \sum_{i=1}^n \sum_{j=1}^n \left\| (\hat{\mathbf{X}}_1 \mathbf{W})_i - (\hat{\mathbf{X}}_2)_j \right\|^2$ is as small as possible. Once we get the final orthogonal matrix $\hat{\mathbf{W}} \in \mathbb{R}^{d \times d}$, we set $\tilde{\mathbf{X}}_1 = \hat{\mathbf{X}}_1 \hat{\mathbf{W}}$.

2.3 Quadratic program

We now formulate a quadratic program to find, for each vertex $v \in V_1$, a collection of vertices $\ell(v) \subset V_2 \setminus S_2$ that are “most similar” to v . Here similarity between $v \in V_1$ and $u \in V_2$ is measured in terms of the Euclidean distances between their embeddings. In other words, given a *query* vertex v in the first graph, our proposed algorithm outputs a nomination list $\ell(v)$ of vertices in the second graph that are most similar to v ; these vertices are deemed “interesting” in the context of the query vertex v .

Our quadratic program is described as follows. Given the aligned embeddings $\tilde{\mathbf{X}}_1$ and $\hat{\mathbf{X}}_2$, we find $\hat{\mathbf{D}}$ to minimize the following objective function

$$\hat{\mathbf{D}} = \arg \min_{\mathbf{D} \in \mathbb{R}^{n \times m}} \sum_{i=1}^n \sum_{j=1}^m \left\| (\tilde{\mathbf{X}}_1)_i - (\hat{\mathbf{X}}_2)_j \right\|_2 \cdot \mathbf{D}_{i,j} + \lambda \|\mathbf{D}\|_F^2, \quad (1)$$

subject to the constraints that

- (i) $\sum_{j=1}^m \mathbf{D}_{i,j} = m$, for all $1 \leq i \leq n$,
- (ii) $\sum_{i=1}^n \mathbf{D}_{i,j} = n$, for all $1 \leq j \leq m$,
- (iii) $\mathbf{D}_{i,j} \geq 0$, for all $1 \leq i \leq n, 1 \leq j \leq m$,
- (iv) $\mathbf{D}_{(S_1)_k, (S_2)_k} = \min\{n, m\}$, for all $1 \leq k \leq K$.

Here $\left\| (\hat{\mathbf{X}}_1)_i - (\hat{\mathbf{X}}_2)_j \right\|$ is the Euclidean distance between the i th vertex’s embedding of G_1 and the j th vertex’s embedding of G_2 , $\lambda > 0$ is a penalty parameter, and $(S_1)_k, (S_2)_k$ represents the index of the k th seed vertex in G_1 and G_2 , respectively.

The motivation behind solving the above optimization problem is as follows. The constraints on \mathbf{D} state that (1) each vertex $i \in V_1$ is mapped to some collection of vertices in $j \in V_2$, namely those for which $\hat{\mathbf{D}}_{ij} > 0$ (constraint iii.); (2) since for any $i \in V_1$, $\sum_j \hat{\mathbf{D}}_{ij} = m$ where $m = |V_2|$, larger values of $\hat{\mathbf{D}}_{ij}$ indicates more “similarity” between

$i \in V_1$ and $j \in V_2$ (constraints i. and ii.); and (3) a seed vertex $s \in S_1$ will get mapped to its unique correspondence $\sigma(s) \in S_2$ (constraint iv.).

We now consider the objective function. The first part of the objective function indicates that the similarity between the i th vertex in V_1 and the j th vertex in V_2 is based on the Euclidean distance $\|(\tilde{\mathbf{X}}_1)_i - (\hat{\mathbf{X}}_2)_j\|$, i.e., larger distance should lead to smaller $\hat{\mathbf{D}}_{ij}$. We can then consider, for each $i \in V_1$, the nomination list for i as being the vertices in $V_2 \setminus S_2$ arranged according to decreasing values of $\{\hat{\mathbf{D}}_{ij}\}_{j \in V_2 \setminus S_2}$. The second part of the objective function, i.e., the penalty term $\lambda \|\mathbf{D}\|_F^2$, is to discourage sparsity of $\hat{\mathbf{D}}$. More specifically, removal of the penalty term $\lambda \|\mathbf{D}\|_F^2$ leads to a linear programming problem for which the minimizer $\hat{\mathbf{D}}$ may lie on the boundary of the feasibility region, i.e., the elements of $\hat{\mathbf{D}}$ take values only in $\{0, m, n\}$. If $\hat{\mathbf{D}}_{i,j} = m$, then the i th vertex in V_1 is mapped to the j th vertex in V_2 and if $\hat{\mathbf{D}}_{i,j} = n$ then the j th vertex in V_2 is mapped to the i th vertex in V_1 . This gives a nomination list with a single candidate. This type of nomination list, when accurate, can significantly reduce the burden of post-processing and checking/verifying multiple candidates. However, it is also likely to be non-robust. By adding the penalty term, we encourage the elements in each row of $\hat{\mathbf{D}}$ to be more uniform since, for any vector $x \in \mathbb{R}^m$, $\|x\|_{\ell_2} \geq m^{-1/2} \|x\|_{\ell_1}$ with equality if and only if all the elements of x are the same. We note that the optimization problem in Eq. (1) is analogous to the *quadratically regularized* optimal transport problem between the point masses induced by $\tilde{\mathbf{X}}_1$ and $\hat{\mathbf{X}}_2$.

The resulting optimization problem is a quadratic program with linear constraints, and the coefficient matrix of the quadratic term is positive definite. Thus, for a fixed $\lambda > 0$, the optimization function is strongly convex and hence there exists a *unique* global minimizer $\hat{\mathbf{D}}$ for any given $\tilde{\mathbf{X}}_1$ and $\hat{\mathbf{X}}_2$. In particular, for a fixed $\lambda > 0$, the solution $\hat{\mathbf{D}}_\lambda$ of Eq. (1) is of the form (Blondel et al., 2018)

$$\hat{\mathbf{D}}_\lambda(i, j) = \frac{1}{\lambda} \left[\|(\tilde{\mathbf{X}}_1)_i - (\hat{\mathbf{X}}_2)_j\| - \hat{\alpha}_i - \hat{\beta}_j \right]_+,$$

where $[z]_+ = \max\{z, 0\}$, and $\hat{\boldsymbol{\alpha}} = (\hat{\alpha}_1, \dots, \hat{\alpha}_n)$ and $\hat{\boldsymbol{\beta}} = (\hat{\beta}_1, \dots, \hat{\beta}_m)$ solve the unconstrained dual problem

$$\max_{\boldsymbol{\alpha} \in \mathbb{R}^n, \boldsymbol{\beta} \in \mathbb{R}^m} n\boldsymbol{\alpha}^\top \mathbf{1} + m\boldsymbol{\beta}^\top \mathbf{1} - \frac{1}{2\lambda} \sum_{i=1}^n \sum_{j=1}^m \left[\|(\tilde{\mathbf{X}}_1)_i - (\hat{\mathbf{X}}_2)_j\| - \alpha_i - \beta_j \right]_+.$$

The optimal solution can be found, theoretically, in polynomial time using the ellipsoid algorithm of [Kozlov et al. \(1980\)](#). In practice we use the Gurobi solver ([Incorporated, 2015](#)), which is based on an interior-point algorithm.

There is no simple and universal approach for choosing λ in practice. If there are seed vertices, then we can do cross-validation by leaving out a subset (or all) of the seed vertices and choose λ for which the nomination on the seed vertices has smallest MRR or MNR. In general, as vertex nomination is an unsupervised learning problem, the issue of choosing tuning parameter is, in a sense, unsolved (at least without additional information such as having seed vertices or a known collection of pair of vertices that should not be matched together). Nevertheless, we note that, empirically, the nomination list found by our algorithm is *not* overly sensitive to the choice of the λ , as λ mainly influences the magnitudes of the elements in $\hat{\mathbf{D}}$ but does not changes their relative ordering too much.

The quadratic program considered in Eq. (1) is motivated by the two-dimensional linear assignment problem. The most obvious formulation of the current vertex nomination problem to three or more graphs will lead to an optimization problem that is similar to the multi-dimensional assignment problem ([Pierskalla, 1968](#)), which is NP-hard. We thus leave the detailed study of multi-sample vertex nomination for future work.

2.4 Computational complexity

We now describe the computational complexity for our proposed algorithm. Firstly, the embedding step is roughly $O((n^2 + m^2)d)$ where d is the embedding dimension ([Huffel, 1990](#)) and n and m are the number of vertices in the first and second graph, respectively. The orthogonal Procrustes is roughly $O(\min\{m, n\}d^2)$. The adaptive point set registration can be done iteratively with each iteration having computational complexity of $O(2^d nmd)$, and generally speaking $\ell \leq 50$ iterations suffice from empirical observations. The solution of the quadratic programming problem can also be solved iteratively with each iteration having a complexity of $O(nm)$ operations; the number of iterations is (empirically) generally bounded and is also independent of the data dimension. As such, the expected empirical complexity of the quadratic programming step is also $O(nm)$ ([Dessein et al., 2018](#)).

Empirically, we record the running time of the simulation experiments in Section 4.1 on $n = 300$ vertices and $n = 1000$ vertices, respectively (here we set $m = n$). For our algorithm with orthogonal Procrustes, the **total** running time for the experiments on $n = 300$ vertices for various choices of ρ (Figure 1 or Figure 2) is about 2 hours while the total running time for $n = 1000$ vertices (Figure C10 or Figure C11 in Appendix C) is about 23 hours. The running time of our algorithm with the adaptive point set registration procedure also has the similar ratio. In summary, we see that the running time of our algorithm does scale (approximately) quadratically with n , the number of vertices, which is consistent with the above analysis.

3 Theoretical Results

We now investigate the theoretical properties of our proposed algorithm. For simplicity we will only consider the case where G_1 and G_2 have the same number of vertices; the analysis presented here will also extend to the case when G_1 and G_2 have different number of vertices provided that the number of common vertices is sufficiently large. We first formulate a generative model for generating pairs of random graphs (G_1, G_2) with underlying latent correspondence σ between the vertices V_1 of G_1 and V_2 of G_2 . We then show consistency results about our scheme under the generative model and analyze the accuracy of the nomination list obtained by our algorithm. We next investigate the impact of having seed vertices. In particular, we propose a procedure for re-ranking the nomination lists in the presence of seed vertices. The empirical results in Section 4 indicates that if the number of seed vertices is not too small, then this optional re-ranking step outputs an improved nomination list $\ell(x)$ compared to the nomination list obtained directly from the quadratic program solution.

Our generative model for pairs of random graphs depends on the following notion of the generalized random dot product graphs (Rubin-Delanchy et al., 2017; Young and Scheinerman, 2007).

Definition 1 (Generalized random dot product graphs). Let $d \geq 1$ be given and let \mathcal{X} be

a subset of \mathbb{R}^d such that $x^\top \mathbf{I}_{p,q} y \in [0, 1]$. Here $\mathbf{I}_{p,q}$ is a $d \times d$ diagonal matrix with diagonal entries containing p “+1” and q “-1” for integers $p, q \geq 0, p + q = d$. For a given $n \geq 1$, let \mathbf{X} be a $n \times d$ matrix with rows $X_i \in \mathcal{X}$ for $i = 1, 2, \dots, n$. A random graph G is said to be an instance of a generalized random dot product graph with latent positions \mathbf{X} if the adjacency matrix \mathbf{A} of G is a symmetric matrix whose upper triangular entries $\{\mathbf{A}(i, j)\}_{i \leq j}$ are independent Bernoulli random variables with

$$\mathbf{A}(i, j) \sim \text{Bernoulli}(X_i^\top \mathbf{I}_{p,q} X_j).$$

We use $\text{GRDPG}(\mathbf{P})$ to represent such graph, where $\mathbf{P} = \mathbf{X} \mathbf{I}_{p,q} \mathbf{X}^\top$.

Generalized random dot product graphs are a special case of latent position graphs or graphons (Diaconis and Janson, 2008; Hoff et al., 2002; Lovász, 2012). In the general latent position graph model, each vertex v_i is associated with a latent or unobserved vector X_i and, given the collection of latent vectors $\{X_i\}$, the edges are conditionally independent Bernoulli random variables with $\mathbb{P}[v_i \sim v_j] = \kappa(X_i, X_j)$ for some *symmetric* link function κ . Generalized random dot product graphs can be used to model any latent position graphs where the link function κ is finite-dimensional, i.e., κ is such that for any n and for any collection of latent vectors $\{X_i\}_{i=1}^n$, the $n \times n$ matrix \mathbf{P} with $\mathbf{P}(i, j) = \kappa(X_i, X_j)$ has rank at most d for some *arbitrary* but fixed d not depending on n . Indeed, as \mathbf{P} is a symmetric matrix with rank at most d , \mathbf{P} has an eigendecomposition as $\mathbf{P} = \mathbf{U} \mathbf{\Lambda} \mathbf{U}^\top$. Hence, taking $\mathbf{X} = \mathbf{U} |\mathbf{\Lambda}|^{1/2}$ and letting p and q be the number of positive and negative eigenvalues of \mathbf{P} , we obtained a representation of \mathbf{P} as a GRDPG.

Generalized random dot product graphs include, as special cases, the popular class of stochastic block model graphs and their degree-corrected and mixed-membership variants (Airoldi et al., 2008; Holland et al., 1983; Karrer and Newman, 2011).

Definition 2. (Stochastic block model random graphs). We say a random graph G with adjacency matrix \mathbf{A} is distributed as a stochastic block model random graph with parameters L, b, \mathbf{B} if

1. The vertex set V of G is partitioned into L blocks, $V = V_1 \cup V_2 \cup \dots \cup V_L$.

2. The function b is a mapping from V to $\{1, \dots, L\}$ with $b(i)$ denoting the block label of vertex $i \in V$.
3. The matrix $\mathbf{B} \in [0, 1]^{L \times L}$ is a symmetric matrix of block probabilities. More specifically, given b , the entries $\mathbf{A}(i, j)$ for $i \leq j$ are *conditionally independent* Bernoulli random variables with $\mathbf{A}(i, j) \sim \text{Bernoulli}(\mathbf{B}_{b(i), b(j)})$.

We denote a stochastic block model graph as $G \sim \text{SBM}(L, b, \mathbf{B})$.

A L -blocks stochastic block model graph (Holland et al., 1983) corresponds to a GRDPG where \mathcal{X} is a mixture of L point masses. Similarly, a L -blocks degree-corrected stochastic block model and a L -blocks mixed-membership stochastic block model correspond to a GRDPG where \mathcal{X} is supported on a mixture of L rays and on a convex hull of L points, respectively. See Rubin-Delanchy et al. (2017) for a more detailed description of these relationships. The perspective of representing a mixed membership SBM as a GRDPG also gives us a general approach to constructing the domain \mathcal{X} for a GRDPG in Definition 1. More specifically, we can construct \mathcal{X} by first finding some collection of K vectors $\mathcal{S} = \{X_1, X_2, \dots\}$ for which $X_i^\top \mathbf{I}_{p,q} X_j \in [0, 1]$ for all $X_i, X_j \in \mathcal{S}$ and then construct \mathcal{X} as the convex hull of the \mathcal{S} .

Our generative model for pairs of random graphs extends the GRDPG model for the single graph setting to the setting of two graphs that share a common set of vertices with edges that are possibly correlated.

Definition 3 (ρ -correlated GRDPG). Assume the notation in Definition 1. Let $\rho \in [-1, 1]$ be given. A *pair* of random graphs (G_1, G_2) is said to be an instance of a ρ -correlated generalized random dot product graphs with latent positions \mathbf{X} if the pair of adjacency matrices \mathbf{A}_1 and \mathbf{A}_2 satisfy the following conditions.

1. Marginally $G_1 \sim \text{GRDPG}(\mathbf{P})$ and $G_2 \sim \text{GRDPG}(\mathbf{P})$.
2. Given \mathbf{P} , the bivariate random variables $\{\mathbf{A}_1(i, j), \mathbf{A}_2(i, j)\}_{1 \leq i < j \leq n}$ are collectively independent and

$$\text{corr}(\mathbf{A}_1(i, j), \mathbf{A}_2(i, j)) = \rho,$$

for any $1 \leq i < j \leq n$.

The correlation ρ in Definition 3 induces a notion of correspondence between the vertices in G_1 and G_2 . More specifically, if $\rho = 0$ then for any two arbitrary pairs of vertices (i, j) and (k, ℓ) , the edges $\mathbf{A}_1(i, j)$ and $\mathbf{A}_2(k, \ell)$ are independent. In contrast, if $\rho \neq 0$ then $\mathbf{A}_1(i, j)$ and $\mathbf{A}_2(k, \ell)$ are independent if and only if $\{i, j\} \neq \{k, \ell\}, \{i, j\} \neq \{\ell, k\}$. Now suppose that $\rho \neq 0$. Then given a vertex of interest $v \in G_1$, we can define the true correspondence of v in G_2 as the *unique* vertex $\sigma(v) \in G_2$ such that the edges $\mathbf{A}_1(v, u)$ and $\mathbf{A}_2(\sigma(v), \sigma(u))$ are correlated *for all* $u \in G_1$. In summary, if (G_1, G_2) is a pair of ρ -correlated GRDPG graphs with $\rho \neq 0$ then there exists a *canonical* correspondence between the vertices of G_1 and the vertices of G_2 . We use this correspondence to define our notion of “interestingness” when evaluating the proposed methodology on graphs generated from the ρ -GRDPG model, i.e., given a query vertex $v \in G_1$, we wish to find $\sigma(v) \in G_2$. See [Agterberg et al. \(2020\)](#); [Lyzinski et al. \(2014\)](#); [Patsolic et al. \(2017\)](#) for further discussion of the relationship between ρ and its induced correspondence in graph matching and vertex nomination problems.

We now state our first theoretical result. The following result provides an error bound for the $2 \rightarrow \infty$ norm difference between the adjacency spectral embeddings of G_1 and G_2 ; given a $n \times p$ matrix \mathbf{M} with rows M_i , the $2 \rightarrow \infty$ norm of \mathbf{M} is the maximum ℓ_2 norm of the rows M_i , i.e.,

$$\|\mathbf{M}\|_{2 \rightarrow \infty} = \max_{\|\mathbf{x}\|=1} \|\mathbf{M}\mathbf{x}\|_{\infty} = \max_{i=1, \dots, n} \|M_i\|.$$

The main feature of the following $2 \rightarrow \infty$ bound is that it is monotone decreasing in both $\rho > 0$ and n , i.e., larger correlation and/or larger number of vertices in each graph lead to smaller error bound that holds *uniformly* for all vertices of G_1 and G_2 . We emphasize that previous bounds for $\min_{\mathbf{W} \in \mathbb{O}_d} \|\hat{\mathbf{X}}_1 \mathbf{W} - \mathbf{X}\|_{2 \rightarrow \infty}$ and $\min_{\mathbf{W} \in \mathbb{O}_d} \|\hat{\mathbf{X}}_2 \mathbf{W} - \mathbf{X}\|_{2 \rightarrow \infty}$ (see e.g., [Rubin-Delanchy et al. \(2017\)](#)) do not depend on the correlation ρ , and thus will lead to a potentially sub-optimal bound of the form

$$\min_{\mathbf{W} \in \mathbb{O}_d} \|\hat{\mathbf{X}}_1 \mathbf{W} - \hat{\mathbf{X}}_2\|_{2 \rightarrow \infty} = O_p(n^{-1/2}).$$

Below, we will characterise the error between asymptotic latent position estimations under the assumption that $\mathbf{P} = \gamma \cdot \mathbf{X} \mathbf{I}_{p,q} \mathbf{X}^\top$ where γ is a sparsity factor.

Theorem 1. Let $(G_1, G_2) \sim \rho\text{-GRDPG}(\mathbf{P})$, where $\mathbf{P} = \gamma \cdot \mathbf{X} \mathbf{I}_{p,q} \mathbf{X}^\top \in [0, 1]^{n \times n}$ is symmetric with $\text{rank}(\mathbf{P}) = p + q = d$. Suppose that 1) $\max_i \sum_j \mathbf{P}_{i,j}(1 - \mathbf{P}_{i,j}) \geq C \log^4 n$ for some universal constant C ; 2) the latent positions satisfy $\frac{1}{n} \sum_{i=1}^n X_i X_i^\top \mathbf{I}_{p,q} \xrightarrow{\text{a.s.}} \Gamma$ as $n \rightarrow \infty$. Here Γ is a fixed $d \times d$ matrix not depending on n . Denote by $\mathbf{A}_1, \mathbf{A}_2 \in \mathbb{R}^{n \times n}$ the adjacency matrices for G_1 and G_2 , respectively. Let $\hat{\mathbf{X}}_1$ and $\hat{\mathbf{X}}_2$ be the adjacency spectral embedding of \mathbf{A}_1 and \mathbf{A}_2 into \mathbb{R}^d , respectively. Then there exists a constant $c > 0$ such that

$$\min_{\mathbf{W} \in \mathbb{O}_d} \left\| \hat{\mathbf{X}}_1 \mathbf{W} - \hat{\mathbf{X}}_2 \right\|_{2 \rightarrow \infty} = (1 - \rho)^{1/2} \cdot O_p(n^{-1/2}) + O_p((\log n)^{2c} n^{-1} \gamma^{-1/2}).$$

Condition (1) in the statement of Theorem 1 is a condition on the *sparsity* of the graph. In particular, Condition (1) is satisfied provided that the *maximum degree* of \mathbf{P} is of order $\Omega(\log^4 n)$. Condition (2) is a condition on the homogeneity of the latent positions \mathbf{X} , i.e., as $n \rightarrow \infty$, the latent positions are sufficiently homogeneous so that their sample second moment matrix $\frac{1}{n} \sum_{i=1}^n X_i X_i^\top \mathbf{I}_{p,q}$ converges. Assuming the above conditions are satisfied, Theorem 1 then implies the existence of an orthogonal \mathbf{W}_* such that for ρ sufficiently bounded away from 1,

$$\|\mathbf{W}_*^\top (\hat{\mathbf{X}}_1)_i - (\hat{\mathbf{X}}_2)_i\| = (1 - \rho)^{1/2} \cdot O_p(n^{-1/2}), \quad \text{for all } i = 1, 2, \dots, n.$$

Suppose we are now given a collection of seed vertices S with $|S| \geq d$, the embedding dimension. Suppose furthermore that the $|S| \times d$ matrices $(\hat{\mathbf{X}}_1)_S$ and $(\hat{\mathbf{X}}_2)_S$ are both of full-column rank, i.e., $(\hat{\mathbf{X}}_1)_S$ and $(\hat{\mathbf{X}}_2)_S$ each contains d linearly independent columns. Then by solving the orthogonal Procrustes problem $\min_{\mathbf{W} \in \mathbb{O}_d} \|(\hat{\mathbf{X}}_1)_S \mathbf{W} - (\hat{\mathbf{X}}_2)_S\|_F$, we will obtain an estimate $\hat{\mathbf{W}}$ of \mathbf{W} that still satisfies the claim in Theorem 1. Indeed, we have

$$\|\hat{\mathbf{W}}^\top (\hat{\mathbf{X}}_1)_j - (\hat{\mathbf{X}}_2)_j\| \leq \|\mathbf{W}_*^\top (\hat{\mathbf{X}}_1)_j - (\hat{\mathbf{X}}_2)_j\| = (1 - \rho)^{1/2} \cdot O_p(n^{-1/2}), \quad \text{for all } j \in S.$$

Now for each $i \notin S$, $(\hat{\mathbf{X}}_1)_i$ and $(\hat{\mathbf{X}}_2)_i$ can be written as a linear combination of $(\hat{\mathbf{X}}_1)_j, j \in S$ and $(\hat{\mathbf{X}}_2)_j, j \in S$, respectively. Hence, by the triangle inequality for vector norms,

$$\|\hat{\mathbf{X}}_1 \hat{\mathbf{W}} - \hat{\mathbf{X}}_2\|_{2 \rightarrow \infty} \leq (1 - \rho)^{1/2} \cdot O_p(n^{-1/2}).$$

In summary, estimates of \mathbf{W}_* using either orthogonal Procrustes or point set registration will yield a transformation $\tilde{\mathbf{X}}_1$ of $\hat{\mathbf{X}}_1$ whose rows are *uniformly* close to the rows of $\hat{\mathbf{X}}_2$.

Thus, for the optimization problem in Eq. (1), the costs $\hat{c}_{ij} = \|(\tilde{\mathbf{X}}_1)_i - (\hat{\mathbf{X}}_2)_j\|$ will be close to $c_{ij} = \|X_i - X_j\|$, i.e.,

$$\max_{i \neq j} |\hat{c}_{ij} - c_{ij}| = O_P(n^{-1/2}), \quad \max_i |\hat{c}_{ii} - c_{ii}| = (1 - \rho)^{1/2} O_P(n^{-1/2}). \quad (2)$$

We now consider the implications of Theorem 1 on the solution of the optimization problem in Eq. (1). Suppose first that $\lambda = 0$ so that the optimization problem in Eq.(1) reduces to a linear programming. Suppose also that $c_{ij} > 0$ whenever $i \neq j$ and $c_{ii} = 0$, i.e., the latent positions $\{X_i\}$ are unique. Then as $n \rightarrow \infty$, by the above bounds for $|\hat{c}_{ij} - c_{ij}|$, we have $\hat{\mathbf{D}}_{i,i} = n$ for all $1 \leq i \leq n$ and hence, for any vertex of interest x in G_1 , our algorithm will give the nomination list with the true $\sigma(x)$ at the top of the list.

We next consider the case where $\lambda > 0$. Define \mathbf{C} and $\hat{\mathbf{C}}$ as the $n \times n$ matrices whose elements are c_{ij} and \hat{c}_{ij} respectively. Let

$$\mathcal{D} = \{\mathbf{D} : \mathbf{D} \in \mathbb{R}_+^{n \times n}, \mathbf{D}\mathbf{1}_n = (n, \dots, n)^\top, \mathbf{D}^\top \mathbf{1}_n = (n, \dots, n)^\top\}.$$

The optimization problem in Eq. (1) is then equivalent to

$$\operatorname{argmin}_{\mathbf{D} \in \mathcal{D}} \langle \hat{\mathbf{C}}, \mathbf{D} \rangle + \lambda \|\mathbf{D}\|_F^2 = \operatorname{argmin}_{\mathbf{D} \in \mathcal{D}} \|\mathbf{D} + \frac{1}{2\lambda} \hat{\mathbf{C}}\|_F^2, \quad \lambda > 0.$$

Let $\hat{\mathbf{D}}_\lambda$ be the *unique* solution of the above problem. Then $\hat{\mathbf{D}}_\lambda$ is the *projection* of $-\frac{1}{2\lambda} \hat{\mathbf{C}}$ onto the convex set \mathcal{D} . Now consider the solution of Eq. (1) where we replaced $\hat{\mathbf{C}}$ by \mathbf{C} and denote that unique solution as \mathbf{D}_λ . From Eq. (2) we have $\|\hat{\mathbf{C}} - \mathbf{C}\|_F^2 = \sum_{ij} (\hat{c}_{ij} - c_{ij})^2 = O_P(n)$ and hence $\|\hat{\mathbf{C}} - \mathbf{C}\|_F = O_P(n^{1/2})$. Next recall that the projection in Frobenius norm onto convex sets is 1-Lipschitz. We therefore have

$$\|\mathbf{D}_\lambda - \hat{\mathbf{D}}_\lambda\|_F \leq \frac{1}{2\lambda} \|\hat{\mathbf{C}} - \mathbf{C}\|_F = \frac{1}{2\lambda} \cdot O_P(n^{1/2}).$$

Since $\|\mathbf{D}\|_F \geq n$ for all $\mathbf{D} \in \mathcal{D}$, we see that $\|\hat{\mathbf{D}}_\lambda - \mathbf{D}_\lambda\|_F = o(\|\mathbf{D}_\lambda\|)$ for all $\lambda \gg n^{-1/2}$. In other words, provided that λ is not too small, the solutions of Eq. (1) using the true cost matrix \mathbf{C} and using the estimated cost matrix $\hat{\mathbf{C}}$ are close, i.e., the relative error between \mathbf{D}_λ and $\hat{\mathbf{D}}_\lambda$ could be made arbitrarily small for sufficiently large n .

Finally, we consider how the solution \mathbf{D}_λ using the true cost matrix \mathbf{C} will look like as $\lambda \rightarrow 0$. Let P_0 be the linear programming problem $\min_{\mathbf{D} \in \mathcal{D}} \langle \mathbf{C}, \mathbf{D} \rangle$. Suppose n is now fixed.

Then if $\lambda \rightarrow 0$, \mathbf{D}_λ will converge to the optimal solution with *minimum Frobenius norm* among the set of all optimal solutions of P_0 , i.e., letting ξ_* be the minimum objective value of P_0 , we have

$$\mathbf{D}_\lambda \longrightarrow \operatorname{argmin}_{\mathbf{D} \in \mathcal{D}} \{\|\mathbf{D}\|_F : \langle \mathbf{C}, \mathbf{D} \rangle = \xi_*\}.$$

We note that there could be multiple solutions of $\{\mathbf{D} \in \mathcal{D} : \langle \mathbf{C}, \mathbf{D} \rangle = \xi_*\}$. Nevertheless, in the event that P_0 has a *unique* minimizer, then since $c_{ii} = 0$ for all i , this unique minimizer will be given by $\mathbf{D}_* = \operatorname{diag}(n, n, \dots, n)$. Therefore, by the continuity of the optimization problem, there exists a $\lambda > 0$ such that $\mathbf{D}_\lambda = \mathbf{D}_*$. The previous bound for $\|\hat{\mathbf{D}}_\lambda - \mathbf{D}_\lambda\|_F$ thus suggests that $\hat{\mathbf{D}}_\lambda \rightarrow \mathbf{D}_*$ as $\lambda \rightarrow 0$. A precise statement of this result, however, requires a more detailed analysis of the relationship between λ and n . Indeed, the relative error bound for $\|\hat{\mathbf{D}}_\lambda - \mathbf{D}_\lambda\|_F$ currently requires n sufficiently large and $\lambda \gg n^{-1/2}$ while the convergence of \mathbf{D}_λ to \mathbf{D}_* currently requires $\lambda \rightarrow 0$ with n fixed. We leave this analysis for future work. Finally, if we can assume that for sufficiently large n we also have $\min_{i \neq j} c_{ij} = \omega(n^{-1/2})$, then with high probability $\hat{\mathbf{D}}_0 = \operatorname{diag}(n, n, \dots, n)$ and we exactly recover the true correspondence for all vertices. The condition $\min_{i \neq j} c_{ij} = \omega(n^{-1/2})$ is likely to be too restrictive; we can relax this condition by assuming that the indices $\{1, 2, \dots, n\}$ can be partitioned into K distinct groups such that $c_{ij'} > c_{ij} + \omega(n^{-1/2})$ for all triplets (i, j, j') where i and j are in the same group and i and j' are in different groups. Then under this milder condition, we can guarantee that with high probability, $\hat{\mathbf{D}}_0$ satisfies $\hat{\mathbf{D}}_0(i, j) = 0$ whenever i and j are in different groups. As a special case if G_1, G_2 are ρ -correlated stochastic block model graphs then \mathbf{D}_0 will be block-diagonal and hence, for sufficiently large n , $\hat{\mathbf{D}}_0$ will also be block-diagonal with high probability. Thus, for ρ -correlated stochastic block models, our algorithm will generally assign each vertex $u \in G_1$ to another vertex $v \in G_2$ from the same block as u .

We summarize the above discussion in the following result.

Proposition 1. *Let P_λ and \hat{P}_λ be the optimization problem in Eq. (1) with cost matrices $\mathbf{C} = (\|X_i - X_j\|)$ and $\hat{\mathbf{C}} = (\|\hat{\mathbf{W}}(\tilde{\mathbf{X}}_1)_i - (\tilde{\mathbf{X}}_2)_j\|)$, respectively. Then for sufficiently large n ,*

$$\frac{\|\mathbf{D}_\lambda - \hat{\mathbf{D}}_\lambda\|_F}{\|\mathbf{D}_\lambda\|_F} = \frac{1}{\lambda} \cdot O_p(n^{-1/2}).$$

For a fixed n , as $\lambda \rightarrow 0$, we have

$$\mathbf{D}_\lambda \longrightarrow \operatorname{argmin}_{\mathbf{D} \in \mathcal{D}} \{\|\mathbf{D}\|_F : \langle \mathbf{C}, \mathbf{D} \rangle = \xi_*\},$$

where ξ_* is the minimum value achieved in P_0 . Furthermore, suppose that $\lambda = 0$ and, for sufficiently large n the vertices of G_1 and G_2 can be partitioned into K distinct groups such that $c_{ij} < c_{ij'}$ with $c_{ij'} - c_{ij} = \omega(n^{-1/2})$ for all triplets (i, j, j') with i and j being the same group and i and j' being in different groups. Then with high probability $\hat{\mathbf{D}}_0$ is a block diagonal matrix, i.e., $\hat{\mathbf{D}}_0(i, j) = 0$ whenever i and j are in different groups.

Note that the simulation results in Section 4 are more accurate than what Proposition 1 suggests, i.e., the correlation structure between the two graphs lead to better nomination than just nominating vertices from the same block.

3.1 Reranking based on likelihood

The algorithm in Section 2 output a nomination list $\ell(x)$ for the vertex of interest. When the pair (G_1, G_2) is an instance of a ρ -correlated generalized random dot product graph, then for any fixed $\rho > 0$, Theorem 1 guarantees that $\sigma(x)$ is located at the top of the nomination list $\ell(x)$, i.e., $\operatorname{rk}(\sigma(x))/n \rightarrow 0$ as $n \rightarrow \infty$, and furthermore, if $\rho = 1$ then $\operatorname{rk}(\sigma(x)) = 1$ asymptotically almost surely.

We now describe a procedure for refining the nomination list so that $\operatorname{rk}(\sigma(x)) = 1$ even when $\rho < 1$, provided that we have enough seed vertices. Let $x \in V_1$ be given and let $v \in V_2$ be arbitrary. Then for any seed vertex $w \in S_1$ with correspondence $\sigma(w) \in S_2$, we have, by the assumptions on the ρ -correlation structure

$$\mathbb{P}(\mathbf{A}_1(x, w) = 1, \mathbf{A}_2(v, \sigma(w)) = 1) = \mathbf{P}(x, w)^2 + \rho \mathbf{P}(x, w)(1 - \mathbf{P}(x, w)), \quad \text{if } v = \sigma(x),$$

$$\mathbb{P}(\mathbf{A}_1(x, w) = 1, \mathbf{A}_2(v, \sigma(w)) = 1) = \mathbf{P}(x, w)\mathbf{P}(v, \sigma(w)), \quad \text{if } v \neq \sigma(x).$$

Let $C_{vw} = \mathbf{A}_1(x, w)\mathbf{A}_2(v, \sigma(w)) \in \{0, 1\}$ and let $p_{vw}(\rho)$ be

$$p_{vw}(\rho) = \mathbf{P}(x, w)\mathbf{P}(v, \sigma(w)) + \rho \mathbf{P}(x, w)(1 - \mathbf{P}(x, w)).$$

Then the collection $\{C_{vw}\}_{w \in S_1}$ are *independent* Bernoulli random variables with mean parameters $\{p_{vw}(\rho)\}_{w \in S_1}$ where $\rho \neq 0$, if and only if $v = \sigma(x)$. For a fixed $\rho \neq 0$, the likelihood

of observing $\{C_{vw}\}_{w \in S_1}$, assuming the edge probabilities $\{\mathbf{P}_{ij}\}_{i < j}$ are known, is then

$$\mathcal{L}(\rho; \{C_{vw}\}_{w \in S_1}) = \prod_{w \in S_1} (p_{vw}(\rho))^{c_{vw}} (1 - p_{vw}(\rho))^{1 - c_{vw}}.$$

Deciding between $v = \sigma(x)$ and $v \neq \sigma(x)$ is thus analogous to test $\mathbb{H}_0: \rho = 0$ against $\mathbb{H}_A: \rho \neq 0$. For our problem, the edge probabilities $\{\mathbf{P}_{i,j}\}_{i < j}$ are unknown. Nevertheless, Theorem 1 guarantees that $\{\mathbf{P}_{i,j}\}_{i < j}$ can be estimated uniformly well by $\{\hat{\mathbf{P}}_{i,j}\}_{i < j}$. In summary, our procedure for refining the nomination list $\ell(x)$ is as follows.

- For every v in top ranked part of $\ell(x)$, find $\hat{\rho}_v \in [-1, 1]$ that maximizes the likelihood $\mathcal{L}(\rho; \{C_{vw}\}_{w \in S_1})$; here the true edge probabilities $\{\mathbf{P}_{i,j}\}$ defining $p_{vw}(\rho)$ are replaced by their estimates $\{\hat{\mathbf{P}}_{i,j}\}_{i < j}$.
- Reorder these $v \in \ell(x)$ according to decreasing values of $|\hat{\rho}_v|$.

4 Simulation and Real Data Experiments

We illustrate the performance of our algorithm by synthetic and real data experiments. For the synthetic data experiments, we generate two types of synthetic data which correspond to two special cases of ρ -correlated GRDPG model. For the real data experiments, we use the high-school friendship data from [Moreno and Neville \(2013\)](#) and Microsoft Bing entity graph transitions data from [Agterberg et al. \(2020\)](#). We evaluate the performance of our algorithm using the following two criteria.

- **Mean reciprocal rank (MRR)**

The reciprocal rank (RR) of a nomination list $\ell(x)$ is a measure of how far down a ranked list one must go to find the true corresponding vertex of interest $\sigma(x)$, i.e., with a slight abuse of notation,

$$\text{RR}(x) = \text{rk}(\sigma(x))^{-1} \in (0, 1],$$

where $\text{rk}(\sigma(x))$ is the rank of $\sigma(x)$ in $\ell(x)$, with ties broken randomly. For Monte Carlo experiments, we also consider the mean reciprocal rank, i.e., the reciprocal rank

averaged over the Monte Carlo replicates; we denote this as MRR. Larger values of RR or MRR indicate better performance.

- **Mean normalized rank (MNR)**

The normalized rank (NR) of a nomination list $\ell(x)$ is another measure of the rank of $\sigma(x)$ in $\ell(x)$, and is defined as

$$\text{NR}(x) = \frac{\text{rk}(\sigma(x)) - 1}{|V_2 \setminus S_2| - 1} \in [0, 1],$$

where $|V_2 \setminus S_2|$ is the set of all possible *non-seed* candidates. Note that $\text{NR}(x) = 0$ if and only if $\text{rk}(\sigma(x)) = 1$. For Monte Carlo experiments we also consider the mean normalized rank (MNR). Smaller values of NR or MNR indicate better performance.

4.1 Simulation experiments

We consider two special cases of the ρ -correlated GRDPG model. We first assume that the matrix of edge probabilities is positive semidefinite, i.e., that $q = 0$ in the GRDPG model. We refer to this as the ρ -RDPG or ρ -correlated random dot product graphs model. The second assumes that the edge probabilities matrix is that of the popular stochastic block model graphs [Holland et al. \(1983\)](#).

In the case of ρ -RDPG, we generate pairs of graphs (G_1, G_2) on $n = 300$ vertices where the latent positions $\{\mathbf{X}_i\}$ are sampled uniformly on the unit sphere in \mathbb{R}^3 . We then choose, uniformly at random, a vertex $x \in V_1$ and use our algorithm to find a nomination list $\ell(x) \subset V_2$. Recall that the edges of the graphs are pairwise correlated. This correlation structure then yields a canonical notion of correspondence between the vertices in G_1 and those in G_2 . In other words, given any vertex $v \in G_1$ with latent position X_v , the most “interesting” or “similar” vertex to v in G_2 is simply the vertex $u \in G_2$ with latent position $X_u = X_v$. We evaluate our algorithm using the mean reciprocal rank (MRR) and the mean normalized rank (MNR) calculated from 500 Monte Carlo replicates. The results, as a function of the correlation $\rho \in \{0, 0.3, 0.5, 0.7, 1\}$, are presented in Figure 1. The embeddings of the graphs are aligned either via orthogonal Procrustes (see Section 2.2) or via the adaptive point set registration procedure of [Myronenko and Song \(2010\)](#).

The setup for ρ -SBM(L, b, \mathbf{B}) is similar. We generate pairs of graphs on $n = 300$ vertices with $L = 3$ blocks and 100 vertices in each block. The block probabilities matrix is

$$\mathbf{B} = \begin{bmatrix} 0.7 & 0.3 & 0.4 \\ 0.3 & 0.7 & 0.2 \\ 0.4 & 0.2 & 0.7 \end{bmatrix}.$$

The mean reciprocal rank (MRR) and the mean normalized rank (MNR), calculated from 500 Monte Carlo replicates, are given in Figure 2.

For these two settings we choose $d = 3$ for the adjacency spectral embedding step, i.e., we embed the graphs into \mathbb{R}^3 . We recall that our algorithm requires alignment of these embeddings either via orthogonal Procrustes or via an adaptive point set registration. These two choices lead to two slightly different quadratic program formulation. More specifically, as we are embedding into \mathbb{R}^3 , the orthogonal Procrustes procedure needs at least 3 seed vertices to align the embeddings. These seed vertices can then be incorporated into the quadratic program in Section 2.3. In contrast, if the embeddings are aligned using adaptive point set registration, then seed vertices are not necessary and hence the quadratic program is formulated with no seeds. When using orthogonal Procrustes, we also explore the impact of K , the number of seed vertices. We find that increasing K does improve our algorithm, but that the improvement is not overly substantial in the regime where K is small. For example, in the ρ -RDGP setting with $\rho = 0.5$, increasing K from 3 to 9 increases the MRR from 0.28 to 0.37 for the orthogonal Procrustes step, thus, for simplicity of presentation, we fixed $K = 6$ and show the results.

The mean reciprocal rank and mean normalized rank of our algorithm, as a function of the correlation coefficient ρ , are presented in Fig. 1 and Fig. 2. Our algorithm is generally quite accurate. In particular, even when $\rho = 0$ our algorithm still performs substantially better than the baseline. We also note that the performance of orthogonal Procrustes (using $K = 6$ seeds) and adaptive point set registration (with no seeds) are similar, with the difference being even less pronounced in the ρ -SBM setting. We posit that the more obvious community structure in the SBM setting helps the adaptive point set registration procedure to align the embeddings more accurately, thereby reducing the need for seed

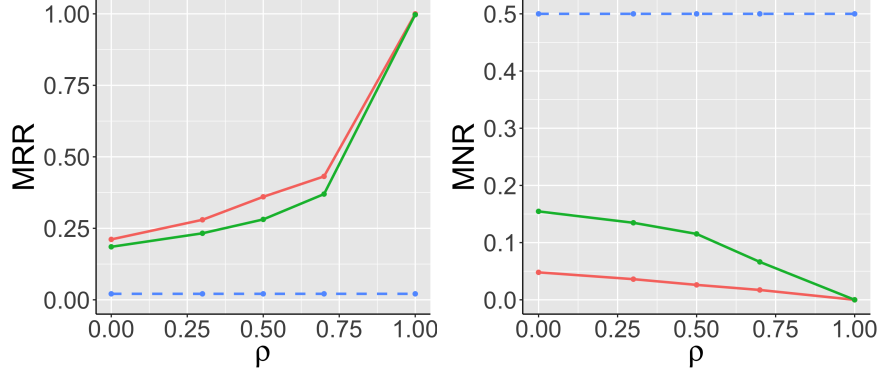


Figure 1: Performance of our algorithm for pairs of ρ -RDPG graphs on $n = 300$ vertices. The mean reciprocal rank (MRR) and mean normalized rank (MNR) are computed based on 500 Monte Carlo replicates. The MRR and MNR are plotted for different values of the correlation coefficient ρ . The red and green lines correspond to the case where the graphs embeddings are aligned via orthogonal Procrustes and via the adaptive point set registration procedure, respectively. The dotted blue lines correspond to the baseline MRR and MNR for a nomination list chosen uniformly at random.

vertices.

We next explore how the reranking step in Section 3.1 can improve the performance of our algorithm, especially when there are enough seed vertices. More specifically, we set $\rho = 0.7$ and vary the number of seed vertices K from 10 to 50. These seed vertices are incorporated into both the quadratic program formulation and the reranking step. We then compare the performance of our algorithm with and without the reranking step. The MRR averaged over 500 Monte Carlo replicates are presented in Fig. 3 for the ρ -RDPG setting and in Fig. 4 for the ρ -SBM setting. These figures indicate that the reranking step leads to significant improvement even for small values of K , e.g., compare the MRR in the ρ -SBM setting with $K = 10$ seeds.

Appendix C contains additional simulation results illustrating how the choice of embedding dimension d , the sparsity parameter γ , and the penalty parameter λ affects the performance of our algorithm. In particular, Figure C1 and Figure C2 show that our algorithm is relatively robust to the choice of d while Figure C5, Table C2 and Table C3

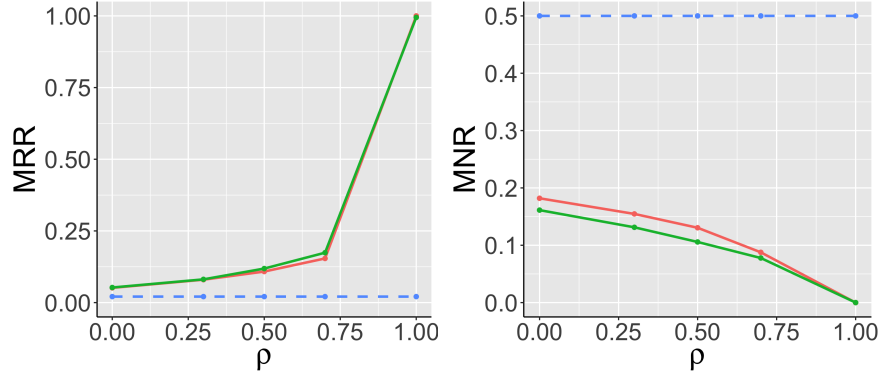


Figure 2: Performance of our algorithm for pairs of ρ -SBM graphs on $n = 300$ vertices. The mean reciprocal rank (MRR) and mean normalized rank (MNR) are computed based on 500 Monte Carlo replicates. See the caption to Figure 1 for further descriptions of the various colored lines.

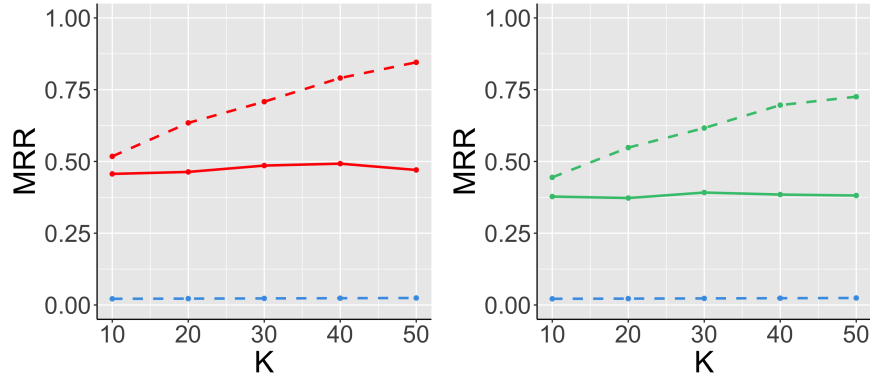


Figure 3: Performance of our algorithm with and without the reranking step for pairs of ρ -RDPG graphs on $n = 300$ vertices and correlation $\rho = 0.7$. The mean reciprocal rank (MRR) are computed based on 500 Monte Carlo replicates. The red and green lines correspond to the case where the graphs embeddings are aligned via orthogonal Procrustes and via the adaptive point set registration procedure, respectively. In each plot, the corresponding dashed red or green line describes the result after the reranking step. The dotted blue lines correspond to the baseline MRR for a nomination list chosen uniformly at random.

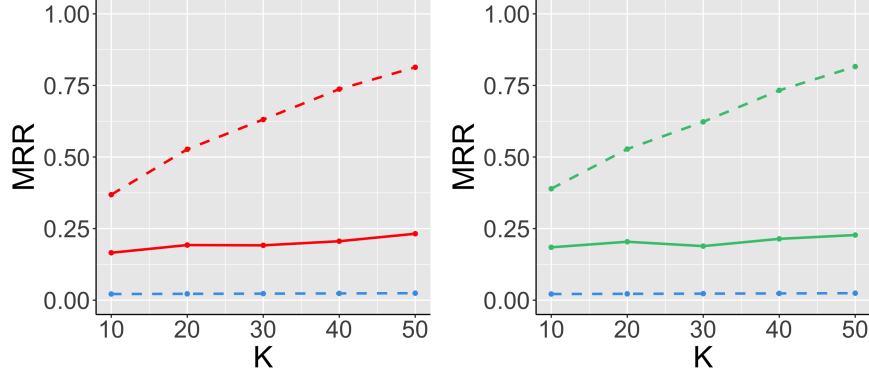


Figure 4: Performance of our algorithm with and without the reranking step for pairs of ρ -SBM(\mathbf{X}) graphs on $n = 300$ vertices and correlation $\rho = 0.7$. See the caption to Figure 3 for further descriptions.

show that our algorithm is also relatively robust to the choice of γ and λ , respectively. In addition, we also include in Appendix C comparisons between our algorithm and the embedding followed by Gaussian mixture modeling algorithm of Agterberg et al. (2020), and we see from Figure C7 and Figure C8 that the accuracy of Agterberg et al. (2020)’s method and our algorithm with orthogonal Procrustes are very similar but we note the running time of Agterberg et al. (2020)’s method is roughly 6 times slower than ours, and we see our algorithm with the adaptive point set registration procedure needs no seeds information but also has comparable accuracy.

4.2 Real data experiments

We now explore the practical application of our algorithms on real data. In Section 4.2.1, we consider a pair of high-school friendship networks containing some of the same vertices and in which we would like to identify the same individuals across the two networks. In Section 4.2.2, we explore the graphs derived from Microsoft Bing entity graph transitions.

4.2.1 High school friendship networks

We first focus on the high school friendship network data from Mastrandrea et al. (2015). This dataset contains two observed graphs and, for each graph, the vertices represent

students and the edges represent their friendship. The first graph is extracted from the Facebook social network, i.e., if two individuals are friends on Facebook, then they are adjacent. The second graph is created based on the result of a survey of the students; for every pair of students, they are considered adjacent if at least one of the students in this pair reports that they are friends with another student. There are 156 vertices in the first graph, 134 vertices in the second graph, and 82 vertices shared between the two graphs. These 82 shared vertices will induce the notion of interestingness for our subsequent analysis. In other words, given a query vertex x in one graph, with x being one of the 82 shared vertices, we are interested in finding the same vertex x in the second graph. This application is thus analogous to that of network deanonymization.

As the number of unshared vertices is reasonably large, we consider two experimental setups. In the first setup we used only the subgraphs induced by the 82 shared vertices while in the other setup we used the full graphs on 156 and 134 vertices. For the adjacency spectral embedding step we set $d = 2$. Orthogonal Procrustes alignment of the embeddings then requires at least 2 seed vertices.

For the experiment using only the shared vertices we iteratively consider each vertex as the vertex of interest. For each vertex of interest we choose a pair of seed vertices, align the embeddings using orthogonal Procrustes, and then solve a quadratic program to obtain a nomination list (the seed vertices are not used in the quadratic program). We repeat this procedure 100 times for each vertex of interest, each time choosing a random pair of seed vertices. Figure 5 then illustrates, for each of the 82 possible vertex of interest x , how often $\text{NR}(x) \in \{0, (0, 0.2], (0.2, 0.5], (0.5, 1]\}$; the mean normalized rank for a nomination list chosen uniformly at random is 0.5. Figure 5 indicates that the nomination lists obtained by our algorithm are in general quite accurate; indeed, the normalized rank values are small for most of the nomination lists, with a significant portion of the nomination lists even having normalized rank values of 0, i.e., the true correspondence of the vertex of interest is at the top of the nomination list.

We next consider the impact of increasing the number of seed vertices K . For simplicity, we present our analysis for a randomly chosen vertex of interest $x = 27$ as an example. Sim-

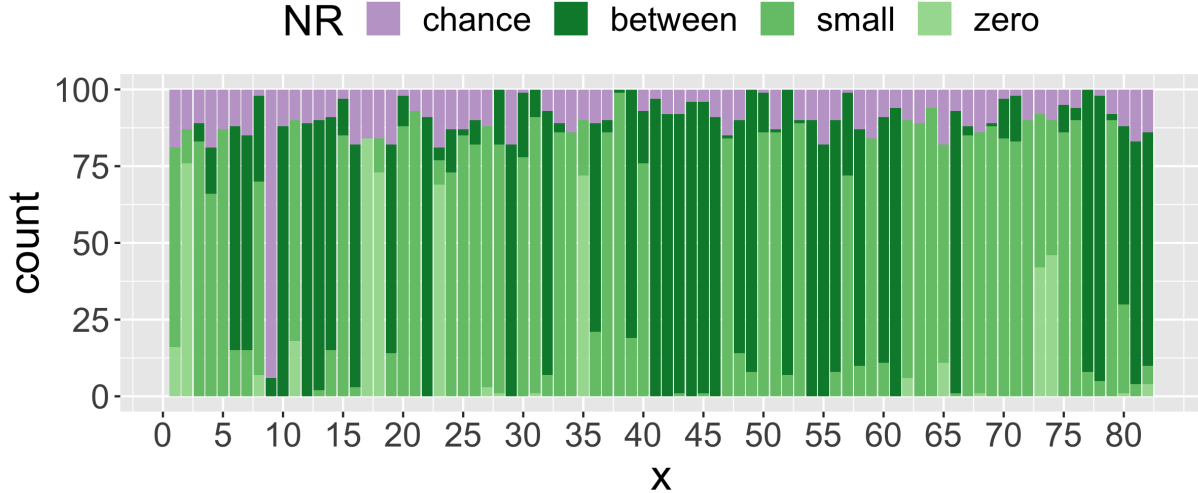


Figure 5: Performance of our algorithm for vertex nomination between the two high-school networks. Here we consider only the subgraphs induced by the 82 shared vertices. The graphs embeddings are aligned via orthogonal Procrustes transformation using two randomly selected seeds; these seeds are only used for the alignment and are not incorporated into the quadratic programming step. For each $x \in V_1$ we repeat this random seeds selection 100 times and record the normalized rank of its correspondence $\sigma(x) \in V_2$. The four categories correspond to the case when the normalized rank (NR) is equal to 0, lying between 0 and 0.2, lying between 0.2 and 0.5, or larger than 0.5.

ilar results hold for other vertices. We vary K from 2 to 10 and run 500 Monte Carlo replicates to compute the MNR. We tabulate how often $\text{NR}(x) \in \{0, (0, 0.2], (0.2, 0.5], (0.5, 1]\}$ in Figure 6. We see from Figure 6 that $K = 7$ seed vertices is sufficient for the NR of the nomination lists for $x = 27$ to be between 0 and 0.2 always.

Analogous results are available when we align the embeddings using adaptive point set registration procedure. However, since adaptive point set registration does not use any seed vertex, it lead to more robust performance when compared to using orthogonal Procrustes. Finally, we note in passing that our algorithm is quite computationally efficient, e.g., generating Figure 5 takes us only about 7 minutes on a normal laptop.

We now consider the setup using the full graphs on 134 and 156 vertices. Once again we use orthogonal Procrustes to align the embeddings. We then consider each of the 82

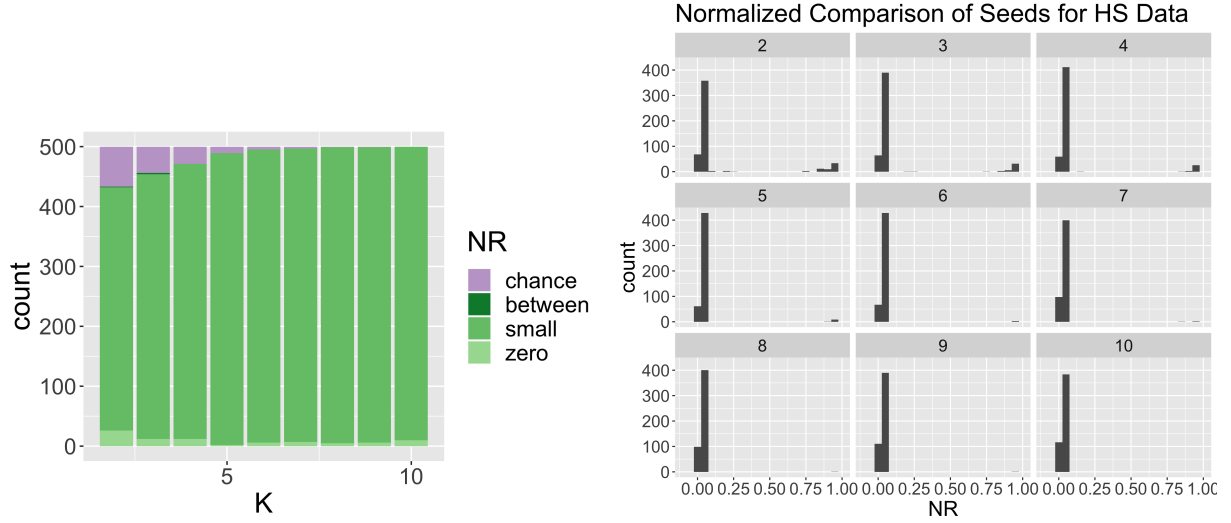


Figure 6: For applying the algorithm with orthogonal Procrustes to subgraphs of high school network generated by shared vertices, using $x = 27$ as the vertex of interest, we vary the number of seed vertices K from 2 to 10, uniformly at random generate 500 sets of seed vertices and plot NR.

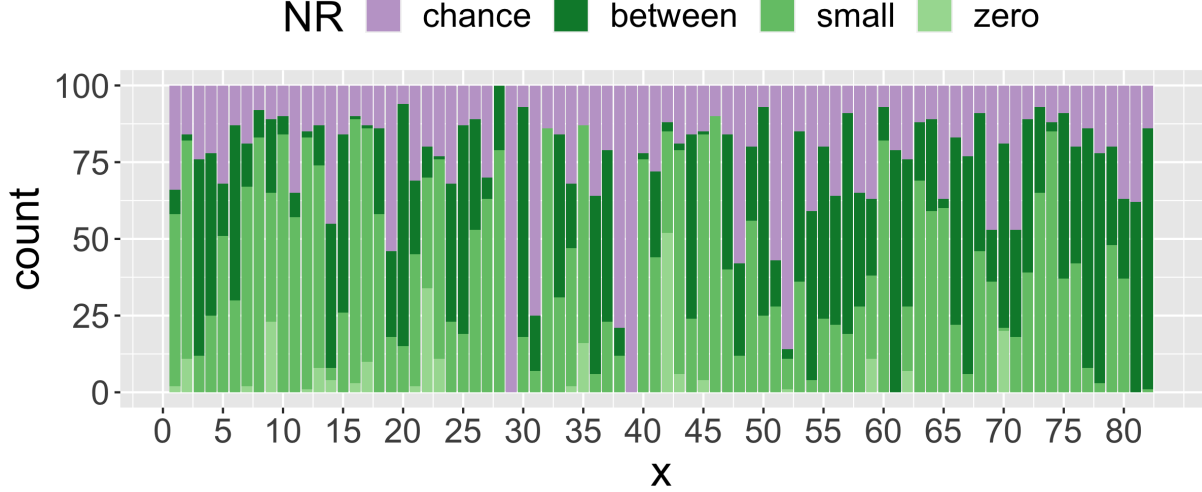


Figure 7: Performance of our algorithm for vertex nomination between the two high-school networks. Here we consider the graphs with full vertices. The graphs embeddings are aligned via orthogonal Procrustes transformation using two randomly selected seeds; these seeds are only used for the alignment and are not incorporated into the quadratic programming step. See the caption to Figure 5 for further descriptions of the experiment.

shared vertices as the vertex of interests x and find the nomination list $\ell(x)$ using the same procedure as that outlined above for the setup using the induced subgraphs. Note that the main difference between the current setup and that of the induced subgraphs is that, for each vertex of interest, there are more candidate vertices in the current setup; this make the task harder and hence the performance of our algorithm is likely to be worse in the current setup. The experiment results in Figure 7 confirmed this speculation. Indeed, comparing Figure 5 and Figure 7, we see that the number of times in which the obtained nomination list is no better than chance increases. Nevertheless, our algorithm is still quite accurate since, for almost all of the vertex of interests, the true correspondences do appear frequently at the top of the nomination lists.

4.2.2 Microsoft Bing entity graph transitions

In this section, we consider graphs derived from one month of Bing entity graph transitions. The dataset for this example is from [Agterberg et al. \(2020\)](#) and contains two graphs on the *same* set of vertices; these vertices denote entities. The (weighted) edges in each graph represent transition rates between the entities during an internet browsing session, but the types of transitions differ between the two graphs. More specifically, the edges in the first graph G_1 represents transitions that were made using a suggestion interface while the transitions in the second graph G_2 were made independently of any suggestion interface. As the suggestion interface can only suggest a few entities at a time, the edges in G_1 are much more constrained than those in G_2 . The first and second graphs both have 13535 vertices and approximately 5.2×10^5 and 5.9×10^5 edges, respectively. There is, once again, a one-to-one correspondence between the vertices in both networks and we use this correspondence to define our notion of interestingness, i.e., given a vertex x in one graph, we are interested in finding the same vertex in the other graph.

For our first analysis we sub-sample the graphs and only consider the subgraphs induced by the first 1000 vertices. These induced subgraphs are also unweighted, i.e., two vertices are adjacent in a induced subgraph if the corresponding transition rate in the original graph is non-zero. Denoting by G_1 and G_2 the resulting induced subgraphs, G_1 and G_2 have 8365

edges and 10247 edges, respectively. We emphasize that there is a 1-to-1 correspondence between the vertex sets of G_1 and G_2 .

We now explore the performance of our algorithm for vertex nomination between G_1 and G_2 . In particular, we sequentially consider each vertex $x \in G_1$ as the vertex of interest, and for a given vertex of interest we randomly select 10 other vertices as seeds. After computing the NR for all vertices, we present the histogram of NR to show the distribution. The results are given in Figure 8 for both the cases where the graph embeddings are aligned via orthogonal Procrustes and via adaptive point set registration. We emphasize that there are two variants of adaptive rigid point set registration used here. In the first variant the 10 seed vertices are used in the quadratic programming formulation while in the second variant the seed vertices are not used at all. Figure 8 indicates that the normalized rank values are generally quite small and hence the nomination lists returned by our algorithm are accurate. Figure 8 also indicates that there is almost no difference between using orthogonal Procrustes and using adaptive point set registration and, more importantly, our algorithm perform well even when there are no seeds information, i.e., the performance of adaptive point set registration with no seeds is virtually identical to that of orthogonal Procrustes and adaptive point set registrations with 10 seeds. Indeed, Table 1 summarizes the quantiles of the NR for different variants of our algorithm and we see from these quantiles that the performance of the three variants are virtually indistinguishable.

	1%	5%	10%	25%	50%	75%	95%	99%
Procrustes (10 seeds)	0.003	0.013	0.030	0.074	0.196	0.387	0.750	0.870
set registration (10 seeds)	0.002	0.012	0.025	0.073	0.196	0.387	0.757	0.877
set registration (no seeds)	0.002	0.013	0.025	0.073	0.196	0.386	0.757	0.876

Table 1: Quantile levels of normalized rank (NR) values for vertex nomination with the Bing entity networks on $n = 1000$ vertices

For our second analysis we do not sub-sample the graphs and hence G_1 contains 13535 vertices and 519389 edges while G_2 contains the same 13535 vertices and 595047 edges. Once again we sequentially consider each vertex $x \in G_1$ is as the vertex of interest. For a given vertex of interest we randomly select 10 other vertices as seeds. We then take

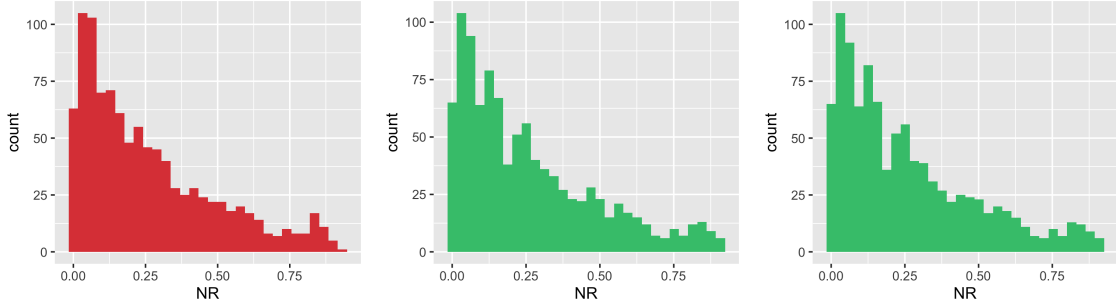


Figure 8: Performance of our algorithm for vertex nomination between the two Microsoft Bing entities transition networks on $n = 1000$ vertices. For each $x \in V_1$ we randomly selected 10 seeds and record the normalized rank (NR) of its correspondence $\sigma(x) \in V_2$. The red and green histogram of NR correspond to the case where the graphs embeddings are aligned via orthogonal Procrustes and via the adaptive point set registration procedure, respectively. The last green figure corresponds to the case for adaptive point set registration procedure without any seeds.

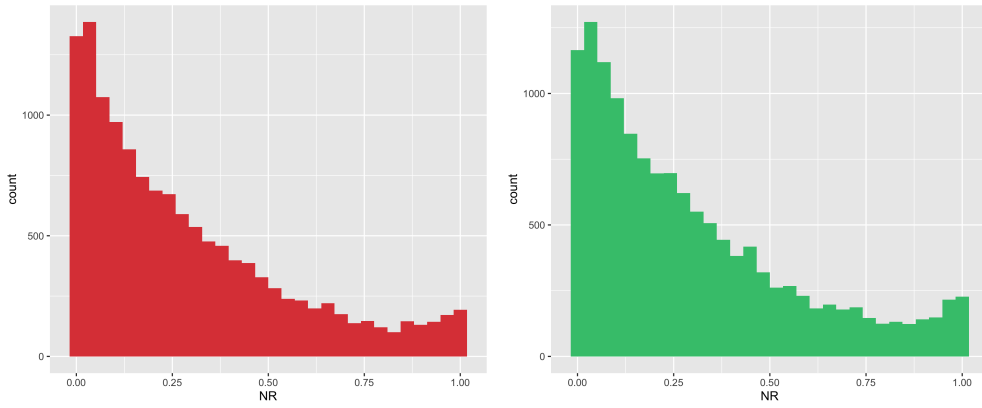


Figure 9: Performance of our algorithm for vertex nomination between the two Microsoft Bing entities transition networks on $n = 13535$ vertices. For each $x \in V_1$ we randomly selected 10 seeds and our algorithms are applied on the 1-neighborhood of them. We record the normalized rank (NR) of its correspondence $\sigma(x)$ in the whole nomination list. The red and green histogram of NR correspond to the case where the graphs embeddings are aligned via orthogonal Procrustes and via the adaptive point set registration procedure, respectively.

the induced subgraph in G_1 (respectively G_2) formed by the 1-neighborhood of these 11 vertices (the vertex of interest and the 10 seed vertices). Letting $G_1(v)$ and $G_2(v)$ denote the induced subgraph of G_1 and G_2 , we then apply our algorithm to find the nomination correspondence $\sigma(x) \in G_2(v)$ for the given vertex of interest $x \in G_1(v)$. The histogram of the NR are summarized in Figure 9. Figure 9 indicates that, even though there is no longer an exact 1-to-1 correspondence between the vertices set in the induced 1-neighborhood subgraphs, our algorithms still give accurate nomination lists.

	1%	5%	10%	25%	50%	75%	95%	99%
Procrustes (10 seeds)	0.000	0.006	0.018	0.073	0.211	0.429	0.869	0.991
set registration (10 seeds)	0.000	0.008	0.022	0.081	0.220	0.440	0.894	0.992

Table 2: Quantile levels of normalized rank (NR) values for vertex nomination with the Bing entity networks on $n = 13535$ vertices

Appendix C contains additional real data analysis results illustrating how the choice of embedding dimension d and the penalty parameter λ affects the performance of our algorithm for the high school friendship data and the Bing data; see Figure C3, Table C1, Figure C4 and Table C4. In addition, Figure C6 and Table C5 illustrate how the reranking step also improves the performance for these real data applications; for example for the Microsoft Bing data, Table C5 in Appendix C.4 shows that with 100 seeds the 25th percentile of the normalized rank changes from 0.073 to 0.027 after we apply the reranking step. It means that without the reranking step, 25% of the time we can find the corresponding vertex among the first 73 vertices of the nomination list, and with the reranking step, 25% of the time we can find the corresponding vertex among the first 27 vertices of the nomination list. This is a substantial improvement and indicates that while we do not expect the Microsoft Bing entity graph transitions data to follow a ρ -correlated GRDPG model, the ρ -correlated GRDPG model still provides a useful surrogate for analyzing the pairwise correlations between the edges of the two Bing graphs. Finally, Appendix C also presents comparisons between our algorithm and the algorithm of Agterberg et al. (2020). For the high school friendship data, we see from Figure C9 that our algorithm is much more accurate and we note the running time of our algorithm with orthogonal Procrustes is only

about 7 minutes compared to their running time which is roughly 200 minutes on the same laptop. Meanwhile, for the Bing data, the algorithm in [Agterberg et al. \(2020\)](#) and our algorithm using either the orthogonal Procrustes alignment or adaptive point set registration alignment have similar normalized rank distribution (see Table C6), but [Agterberg et al. \(2020\)](#) algorithm is roughly 8 times slower than our algorithm.

5 Conclusion

In summary, the current paper provides an algorithm for solving the vertex nomination problem in the multi-graphs setting. Our algorithm depends on adjacency spectral embedding and followed by solving a quadratic programming. To eliminate non-identifiability of spectral embedding for different graphs, besides an approach based on orthogonal Procrustes, we propose a method using adaptive point set registration to align the embedding that also work without needing any information about seed vertices. Under mild assumption, we establish theoretical guarantee on the consistency of our nomination scheme. The empirical results on the simulation and real data analysis demonstrate that our algorithm is generally quite accurate even when there are only a few seeds or even no seed vertices. As we allude to in the introduction of this paper, vertex nomination is an unsupervised learning problem and thus evaluation of a vertex nomination algorithm usually requires some underlying ground truth. The real data analysis examples of this paper are based on pairs of graphs with shared vertices and we used these shared vertices to define our groundtruth; the resulting analysis is thus similar to network deanonymization. When there is no known groundtruth, then our proposed methodology can be used for exploratory data analysis or for suggesting possible matches between a query vertex x in one graph and vertices most “similar” to x in the second graph. To evaluate the accuracy of the resulting nominations will, however, require additional domain knowledge or domain experts. We believe that our chosen examples are simple to describe and yet sufficiently rich in scope, thereby providing a clear and compelling illustration of the effectiveness of our proposed methodology.

While the proposed algorithm is reasonably computationally efficient, there are still technical challenges in applying the algorithm to large graphs. For example, the Bing

graphs analyzed in this paper are on the order of 10^4 vertices and 10^5 to 10^6 edges and our algorithm takes roughly 30 minutes for one full analysis when running on a consumer laptop. For larger-scale graphs, such as those on 10^5 vertices and 10^7 edges, our algorithm breaks down. In particular, the EM steps in the adaptive point set registration algorithm can be quite slow to converge and thus might require sub-sampling of the embedded points before performing the alignment. Furthermore, the quadratic programming step requires keeping track of the assignment matrix \mathbf{D} ; a naive approach of storing \mathbf{D} will require too much memory, especially since \mathbf{D} is likely to be sparse throughout the optimization. Development of iterative procedures for storing and updating \mathbf{D} is thus essential for scaling our algorithm to large graphs. We leave these investigations for future work.

References

- Agterberg, J., Y. Park, J. Larson, C. White, C. E. Priebe, and V. Lyzinski (2020). Vertex nomination, consistent estimation, and adversarial modification. *Electronic Journal of Statistics* 14(2), 3230–3267.
- Ahn, S. C. and A. R. Horenstein (2013). Eigenvalue ratio test for the number of factors. *Econometrica* 81(3), 1203–1227.
- Airoldi, E. M., D. M. Blei, S. E. Fienberg, and E. P. Xing (2008). Mixed membership stochastic blockmodels. *Journal of Machine Learning Research* 9, 1981–2014.
- Blondel, M., V. Seguy, and A. Rolet (2018). Smooth and sparse optimal transport. In *Proceedings of the 21st International Conference on Artificial Intelligence and Statistics*, pp. 880–889.
- Cai, T. T. and A. Zhang (2018). Rate-optimal perturbation bounds for singular subspaces with applications to high-dimensional statistics. *The Annals of Statistics* 46, 60–89.
- Coppersmith, G. A. and C. E. Priebe (2012). Vertex nomination via content and context. arXiv preprint at <http://arxiv.org/abs/1201.4118>.

- Dessein, A., N. Papadakis, and J. Rouas (2018). Regularized optimal transport and the rot mover’s distance. *The Journal of Machine Learning Research* 19(1), 590–642.
- Diaconis, P. and S. Janson (2008). Graph limits and exchangeable random graphs. *Rendiconti di Matematica, Serie VII* 28, 33–61.
- Duch, J. and A. Arenas (2005). Community detection in complex networks using extremal optimization. *Physical Review E* 72, 027104.
- Fishkind, D. E., V. Lyzinski, H. Pao, L. Chen, and C. E. Priebe (2015). Vertex nomination schemes for membership prediction. *Annals of Applied Statistics* 9, 1510–1532.
- Fortunato, S. (2010). Community detection in graphs. *Physics Reports* 486, 75–174.
- Fraley, C. and A. E. Raftery (1998). Mclust: Software for model-based cluster and discriminant analysis. Technical Report 342, Department of Statistics, University of Washington: Technical Report.
- Han, X., Q. Yang, and Y. Fan (2019). Universal rank inference via residual subsampling with application to large networks. *arXiv preprint arXiv:1912.11583*.
- Hoff, P. D., A. E. Raftery, and M. S. Handcock (2002). Latent space approaches to social network analysis. *Journal of the American Statistical Association* 97(460), 1090–1098.
- Holland, P. W., K. B. Laskey, and S. Leinhardt (1983). Stochastic blockmodels: first steps. *Social Networks* 5(2), 109–137.
- Huffel, S. V. (1990). Partial singular value decomposition algorithm. *Journal of computational and applied mathematics* 33(1), 105–112.
- Incorporated, G. O. (2015). Gurobi optimizer reference manual. Available at <http://www.gurobi.com>.
- Karrer, B. and M. E. J. Newman (2011). Stochastic blockmodels and community structure in networks. *Physical Review E* 83(1), 016107.

- Kozlov, M. K., S. P. Tarasov, and L. G. Khachiyan (1980). The polynomial solvability of convex quadratic programming. *USSR Computational Mathematics and Mathematical Physics* 20, 223–228.
- Kudo, T., E. Maeda, and Y. Matsumoto (2005). An application of boosting to graph classification. In *Advances in Neural Information Processing Systems*, pp. 729–736.
- Lee, D. S. and C. E. Priebe (2012). Bayesian vertex nomination. arXiv preprint at <http://arxiv.org/abs/1205.5082>.
- Levin, K. (2017). *Graph Inference with Applications to Low-Resource Audio Search and Indexing*. Ph. D. thesis, Johns Hopkins University.
- Lloyd, J., P. Orbanz, Z. Ghahramani, and D. M. Roy (2012). Random function priors for exchangeable arrays with applications to graphs and relational data. In *Advances in Neural Information Processing Systems*, pp. 998–1006.
- Lovász, L. (2012). *Large networks and graph limits*. American Mathematical Society.
- Lu, L. and X. Peng (2013). Spectra of edge-independent random graphs. *The Electronic Journal of Combinatorics* 20(4), P27.
- Lyzinski, V., D. E. Fishkind, and C. E. Priebe (2014). Seeded graph matching for correlated erdős-rényi graphs. *Journal of Machine Learning Research* 15, 3513–3540.
- Lyzinski, V., K. Levin, D. E. Fishkind, and C. E. Priebe (2016). On the consistency of the likelihood maximization vertex nomination scheme: Bridging the gap between maximum likelihood estimation and graph matching. *Journal of Machine Learning Research* 17, 1–34.
- Lyzinski, V., K. Levin, and C. E. Priebe (2019). On consistent vertex nomination schemes. *Journal of Machine Learning Research* 20, 1–39.
- Mastrandrea, R., J. Fournet, and A. Barrat (2015). Contact patterns in a high school: a comparison between data collected using wearable sensors, contact diaries and friendship surveys. *PLOS One* 10, e0136497.

- Moreno, S. and J. Neville (2013). Network hypothesis testing using mixed kronecker product graph models. In *IEEE 13th International Conference on Data Mining*, pp. 1163–1168.
- Myronenko, A. and X. Song (2010). Point set registration: Coherent point drift. *IEEE Transactions on Pattern Analysis and Machine Intelligence* 32, 2262–2275.
- Newman, M. E. J. (2006). Finding community structure in networks using the eigenvectors of matrices. *Physical Review E* 74, 036104.
- Onatski, A. (2010). Determining the number of factors from empirical distribution of eigenvalues. *The Review of Economics and Statistics* 92(4), 1004–1016.
- Patsolic, H. G., Y. Park, V. Lyzinski, and C. E. Priebe (2017). Vertex nomination via seeded graph matching. arXiv preprint at <http://arxiv.org/abs/1705.00674>.
- Peyré, G. and M. Cuturi (2019). Computational optimal transport. *Foundations and Trends® in Machine Learning* 11(5-6), 355–607.
- Pierskalla, W. P. (1968). The multidimensional assignment problem. *Operations Research* 16(2), 422–431.
- Rubin-Delanchy, P., C. E. Priebe, M. Tang, and J. Cape (2017). A statistical interpretation of spectral embedding: the generalised random dot product graph. arXiv preprint at <http://arxiv.org/abs/1709.05506>.
- Schaeffer, S. E. (2007). Graph clustering. *Computer Science Review* 1, 27–64.
- Schönemann, P. H. (1966). A generalized solution of the orthogonal procrustes problem. *Psychometrika* 31, 1–10.
- Spielman, D. A. and S.-H. Teng (2013). A local clustering algorithm for massive graphs and its application to nearly linear time graph partitioning. *SIAM Journal on Computing* 42, 1–26.
- Sun, M. and C. E. Priebe (2013). Efficiency investigation of manifold matching for text document classification. *Pattern Recognition Letters* 34, 1263–1269.

- Sun, M., M. Tang, and C. E. Priebe (2012). A comparison of graph embedding methods for vertex nomination. In *11th International Conference on Machine Learning and Applications*, pp. 398–403.
- Sussman, D., Y. Park, C. E. Priebe, and V. Lyzinski (2020). Matched filters for noisy induced subgraph detection. *IEEE Transactions on Pattern Analysis and Machine Intelligence* 42, 2887–2900.
- Tang, M., A. Athreya, D. L. Sussman, V. Lyzinski, and C. E. Priebe (2017). A semiparametric two-sample hypothesis testing problem for random dot product graphs. *Journal of Computational and Graphical Statistics* 26, 344–354.
- Xu, J. (2017). Rates of convergence of spectral methods for graphon estimation. arXiv preprint at <http://arxiv.org/abs/1709.03183>.
- Yin, H., A. R. Benson, J. Leskovec, and D. F. Gleich (2017). Local higher-order graph clustering. In *Proceedings of the 23rd ACM SIGKDD International Conference on Knowledge Discovery and Data Mining*, pp. 555–564.
- Yoder, J., L. Chen, H. Pao, E. Bridgeford, K. Levin, D. E. Fishkind, C. Priebe, and V. Lyzinski (2020). Vertex nomination: The canonical sampling and the extended spectral nomination schemes. *Computational Statistics & Data Analysis* 145, 106916.
- Young, S. J. and E. R. Scheinerman (2007). Random dot product graph models for social networks. In *International Workshop on Algorithms and Models for the Web-Graph*, pp. 138–149. Springer.
- Yu, Y., T. Wang, and R. J. Samworth (2014). A useful variant of the Davis–Kahan theorem for statisticians. *Biometrika* 102, 315–323.
- Zhang, M., Z. Cui, M. Neumann, and Y. Chen (2018). An end-to-end deep learning architecture for graph classification. In *32nd AAAI Conference on Artificial Intelligence*, pp. 4438–4445.

Zhu, M. and A. Ghodsi (2006). Automatic dimensionality selection from the scree plot via the use of profile likelihood. *Computational Statistics & Data Analysis* 51, 918–930.

A Proof of Proposition 1

The first part of Proposition 1 has been proved in Section 3. Now we prove the second part, i.e., we will show that for a fixed n , as $\lambda \rightarrow 0$, we have

$$\mathbf{D}_\lambda \longrightarrow \operatorname{argmin}_{\mathbf{D} \in \mathcal{D}} \{\|\mathbf{D}\|_F : \langle \mathbf{C}, \mathbf{D} \rangle = \xi_*\},$$

where ξ_* is the minimum value achieved in P_0 .

The following argument is adapted from the proof of Proposition 4.1 in [Peyré and Cuturi \(2019\)](#). We consider a sequence $(\lambda_\ell)_\ell$ such that $\lambda_\ell \rightarrow 0$ and $\lambda_\ell > 0$. Since \mathcal{D} is bounded, we can extract a sequence (that we do not relabel for the sake of simplicity) such that $\mathbf{D}_{\lambda_\ell} \rightarrow \mathbf{D}_*$. Since \mathcal{D} is closed, $\mathbf{D}_* \in \mathcal{D}$. We consider any \mathbf{D} such that $\langle \mathbf{C}, \mathbf{D} \rangle = \xi_*$. By optimality of such \mathbf{D} and $\mathbf{D}_{\lambda_\ell}$ for their respective optimization problems, we have

$$0 \leq \langle \mathbf{C}, \mathbf{D}_{\lambda_\ell} \rangle - \langle \mathbf{C}, \mathbf{D} \rangle \leq \lambda_\ell \cdot (\|\mathbf{D}\|_F - \|\mathbf{D}_{\lambda_\ell}\|_F). \quad (3)$$

Since $\|\cdot\|_F$ is continuous, taking the limit $\ell \rightarrow +\infty$ in this expression shows that $\langle \mathbf{C}, \mathbf{D}_* \rangle = \langle \mathbf{C}, \mathbf{D} \rangle$ so that \mathbf{D}_* is a feasible point of $\{\mathbf{D} : \langle \mathbf{C}, \mathbf{D} \rangle = \xi_*\}$. Furthermore, dividing by λ_ℓ in Eq. (3) and taking the limit shows that $\|\mathbf{D}_*\|_F \leq \|\mathbf{D}\|_F$, which shows that \mathbf{D}_* is a solution of $\operatorname{argmin}_{\mathbf{D} \in \mathcal{D}} \{\|\mathbf{D}\|_F : \langle \mathbf{C}, \mathbf{D} \rangle = \xi_*\}$.

Finally we prove the claim that if the vertices $\{1, 2, \dots, n\}$ can be partitioned into K distinct groups/blocks such that $c_{ij'} > c_{ij} + \omega(n^{-1/2})$ for all triplets (i, j, j') with i and j being the same group and i and j' being in different groups, then with high probability $\hat{\mathbf{D}}_0$ is block diagonal, i.e., with high probability $\hat{\mathbf{D}}_0(i, j) = 0$ whenever i and j are in different groups.

Suppose that $\hat{\mathbf{D}}_0$ is not block diagonal. Since $n^{-1}\hat{\mathbf{D}}_0$ is a doubly stochastic matrix, by the Birkhoff-von Neumann theorem we can write $n^{-1}\hat{\mathbf{D}}_0$ as a convex combination of permutation matrices, i.e., $\hat{\mathbf{D}}_0 = n \sum_{\sigma} \lambda_{\sigma} \mathbf{\Pi}_{\sigma}$ where the sum is over all permutations σ of $\{1, 2, \dots, n\}$, the $\mathbf{\Pi}_{\sigma}$ represent permutation matrices corresponding to the permutations σ and $\{\lambda_{\sigma}\}$ are the coefficients for the convex combination. We therefore have

$$\langle \hat{\mathbf{C}}, \hat{\mathbf{D}}_0 \rangle = n \sum_{\sigma} \langle \hat{\mathbf{C}}, \lambda_{\sigma} \mathbf{\Pi}_{\sigma} \rangle \geq n \min_{\sigma} \langle \hat{\mathbf{C}}, \mathbf{\Pi}_{\sigma} \rangle. \quad (4)$$

Now according to the condition that $c_{ij'} > c_{ij}$ with $c_{ij'} - c_{ij} = \omega(n^{-1/2})$ for all triplets (i, j, j') where i and j belong to the same group and i and j' belonging to different groups, we have, using Eq. (2), that with high probability $\hat{c}_{ij'} > \hat{c}_{ij}$ for all triplets (i, j, j') satisfying the above groups condition. We will now assume that this condition $\hat{c}_{ij'} > \hat{c}_{ij}$ holds.

We recall that any permutation σ can be decomposed into a product of cycles $\mathcal{C}_1, \mathcal{C}_2, \dots, \mathcal{C}_m$ for some $m \geq 1$. Let \mathcal{C}_r be an arbitrary cycle and suppose that \mathcal{C}_r is of length $s \geq 2$; note that if \mathcal{C}_r has length 1 then \mathcal{C}_r correspond to a fixed point so that $\Pi_\sigma(i, j) = 1$ if and only if $j = i$ where i is the sole index appearing in \mathcal{C}_r . Let i_1 be the smallest index from $\{1, 2, \dots, n\}$ that appears in the cycle \mathcal{C}_r . Then the remaining indices appearing in \mathcal{C}_r are of the form $i_2 = \sigma(i_1), i_3 = \sigma(i_2), \dots, i_s = \sigma(i_{s-1}), i_1 = \sigma(i_s)$. Now if all the indices appearing in \mathcal{C}_r are from the same group then we are done. Otherwise, we split the cycle \mathcal{C}_r into smaller cycles $\{\mathcal{C}_{r1}, \mathcal{C}_{r2}, \dots, \mathcal{C}_{rK}\}$ where each cycle \mathcal{C}_{rk} only have indices appearing in group k . The order of elements in each cycle \mathcal{C}_{rk} are arranged according to the order in which they appear within the original cycle \mathcal{C}_r ; for example if \mathcal{C}_r contains five elements (i_1, i_2, \dots, i_5) with i_1, i_2, i_4 belonging to group 1 and i_3, i_5 belonging to group 2 then $\mathcal{C}_{r1} = (i_1, i_2, i_4)$ and $\mathcal{C}_{r2} = (i_3, i_5)$. Let $\sigma_1, \sigma_2, \dots, \sigma_K$ be the permutations corresponding to these cycles; note that there could be empty cycles \mathcal{C}_{rk} in which case the corresponding σ_k can be dropped or ignored. We then have

$$\sum_{i \in \mathcal{C}_r} \hat{c}_{i\sigma(i)} \geq \sum_{k=1}^K \sum_{i \in \mathcal{C}_{rk}} \hat{c}_{i\sigma_k(i)} \quad (5)$$

with strict inequality unless \mathcal{C}_r only have elements from the same group.

The justification for Eq. (5) is as follows. If i and $\sigma(i)$ are from the same group then $\sigma_k(i) = \sigma(i)$ and hence $\hat{c}_{i\sigma(i)} = \hat{c}_{i\sigma_k(i)}$. Otherwise, if i and $\sigma(i)$ are from different group, say group k and k' , then at the time right before the edge $(i, \sigma(i))$ is considered the index $j = \sigma(i)$ has in-degree 0 and out degree 0 while the index i has in degree 1 and out degree 0. The splitting of \mathcal{C}_r into smaller cycles $\mathcal{C}_{r1}, \dots, \mathcal{C}_{rK}$ is equivalent to changing the outgoing edge for index i and the incoming edge for index $j = \sigma(i)$ using the following rules.

1. If i is the last index in \mathcal{C}_{rk} then we had replace c_{ij} with the strictly smaller cost c_{ii_*} where $i_* = \sigma_k(i)$ is the first index that appears in \mathcal{C}_{rk} . Note that $i_* = i$ is a possibility if \mathcal{C}_{rk} contains only a single index.

2. If i is not the last index in \mathcal{C}_{rk} then we had replace the cost c_{ij} with the strictly smaller cost c_{ii_*} where $i_* = \sigma_k(i)$ is the index appearing right after i in \mathcal{C}_{rk} .
3. If j is the first index in $\mathcal{C}_{rk'}$ then we had replaced c_{ij} with the strictly smaller c_{j_*j} where $j_* = \sigma_{k'}^{-1}(j)$ is the last index that appears in $\mathcal{C}_{rk'}$. There is once again the possibility that $j_* = j$.
4. If j is not the first index in $\mathcal{C}_{rk'}$ then we had replaced c_{ij} with the strictly smaller c_{j_*j} where $j_* = \sigma_{k'}^{-1}(j)$ is the index appearing right before j in $\mathcal{C}_{rk'}$.

Note that in the above steps we neither change the *outgoing* edge of any index i' appearing before i nor change the *incoming* edge of any index j' appearing before j . The sum of the costs c_{ij} for both the incoming and outgoing edges for any cycle \mathcal{C}_r is twice the total cost of the cycle, and hence, by going sequentially through the indices in the cycle \mathcal{C}_r and applying the above rules we will never increase the cost for any outgoing edge or incoming edge; the total sum of the cost for the smaller cycles \mathcal{C}_{rk} is thus strictly less than that for \mathcal{C}_r , with equality if and only if all of the indices appearing in \mathcal{C}_r are from a single group.

The above reasoning implies that the permutation σ_* which minimizes $\langle \hat{\mathbf{C}}, \mathbf{\Pi}_\sigma \rangle$ over all permutation σ is a union of disjoint cycles, each of which contains indices from a single group, i.e., if σ_* minimizes $\langle \hat{\mathbf{C}}, \mathbf{\Pi}_\sigma \rangle$ then $\mathbf{\Pi}_{\sigma_*}(i, j) = 0$ whenever i and j belong to different groups. Let \mathcal{S} be the set of all permutations σ for which $\mathbf{\Pi}_\sigma(i, j) = 0$ whenever i and j belong to different groups. Then by Eq. (4), $\hat{\mathbf{D}}_0 = n \sum_\sigma \lambda_\sigma \mathbf{\Pi}_\sigma$ minimizes $\langle \hat{\mathbf{C}}, \mathbf{D} \rangle$ over the simplex constraint if and only if $\hat{\mathbf{D}}_0$ is a convex combination of elements in \mathcal{S} and hence $\hat{\mathbf{D}}_0(i, j) = 0$ whenever i and j belong to different groups. We had thus justified our last claim from Proposition 1.

B Proof of Theorem 1

The following argument is adapted from the proof of Theorem 5 in [Rubin-Delanchy et al. \(2017\)](#) for bounding $\|\hat{\mathbf{X}} - \mathbf{X}\|_{2 \rightarrow \infty}$ in the case of a *single* generalized random dot product graph to the current setting of bounding $\|\hat{\mathbf{X}}_1 - \hat{\mathbf{X}}_2\|_{2 \rightarrow \infty}$ for a *pair* of *correlated* generalized random dot product graphs.

We set the block spectral decomposition of the symmetric matrix \mathbf{A}_1 as $\mathbf{A}_1 = [\mathbf{U}_1|\mathbf{U}'_1][\mathbf{S}_1 \oplus \mathbf{S}'_1][\mathbf{U}_1|\mathbf{U}'_1]^\top = \mathbf{U}_1\mathbf{S}_1\mathbf{U}_1^\top + \mathbf{U}'_1\mathbf{S}'_1\mathbf{U}'_1{}^\top$, where the diagonal matrix $\mathbf{S}_1 \in \mathbb{R}^{d \times d}$ contains the d largest-in-magnitude nonzero eigenvalues of \mathbf{A}_1 . Similarly, $\mathbf{A}_2 = \mathbf{U}_2\mathbf{S}_2\mathbf{U}_2^\top + \mathbf{U}'_2\mathbf{S}'_2\mathbf{U}'_2{}^\top$. According to the definition of adjacency spectral embedding, we know $\hat{\mathbf{X}}_1 = \mathbf{U}_1|\mathbf{S}_1|^{\frac{1}{2}}$ and $\hat{\mathbf{X}}_2 = \mathbf{U}_2|\mathbf{S}_2|^{\frac{1}{2}}$. So our goal is to prove

$$\min_{\mathbf{W} \in \mathbb{O}_d} \left\| \mathbf{U}_1|\mathbf{S}_1|^{\frac{1}{2}}\mathbf{W} - \mathbf{U}_2|\mathbf{S}_2|^{\frac{1}{2}} \right\|_{2 \rightarrow \infty} = (1 - \rho)^{1/2} \cdot O_p(n^{-1/2}) + O_p((\log n)^{2c} n^{-1} \gamma^{-1/2}).$$

We set $\mathbf{W}^* = \mathbf{W}_1^\top \mathbf{W}_2$, where $\mathbf{W}_1, \mathbf{W}_2$ are two orthogonal matrices and we will give their specific formula in the following proof. Let $\mathbf{P} = \mathbf{U}\mathbf{S}\mathbf{U}^\top$ be the eigendecomposition of \mathbf{P} , where $\mathbf{U} \in \mathbb{R}^{n \times d}$ is the matrix whose columns are the eigenvectors and the diagonal matrix $\mathbf{S} \in \mathbb{R}^{d \times d}$ contains all the d nonzero eigenvalues of \mathbf{P} . Now we split $\mathbf{U}_1|\mathbf{S}_1|^{\frac{1}{2}}\mathbf{W}^* - \mathbf{U}_2|\mathbf{S}_2|^{\frac{1}{2}}$ as

$$\begin{aligned} \mathbf{U}_1|\mathbf{S}_1|^{\frac{1}{2}}\mathbf{W}^* - \mathbf{U}_2|\mathbf{S}_2|^{\frac{1}{2}} &= \underbrace{\left[\mathbf{U}_1|\mathbf{S}_1|^{\frac{1}{2}}\mathbf{W}_1^\top \mathbf{W}_2 - \mathbf{U}\mathbf{U}^\top \mathbf{U}_1|\mathbf{S}_1|^{\frac{1}{2}}\mathbf{W}_1^\top \mathbf{W}_2 \right]}_{\mathbf{T}_1} \\ &\quad + \underbrace{\left[\mathbf{U}\mathbf{U}^\top \mathbf{U}_1|\mathbf{S}_1|^{\frac{1}{2}}\mathbf{W}_1^\top \mathbf{W}_2 - \mathbf{U}|\mathbf{S}|^{\frac{1}{2}}\mathbf{U}^\top \mathbf{U}_1\mathbf{W}_1^\top \mathbf{W}_2 \right]}_{\mathbf{T}_2} \\ &\quad + \underbrace{\left[\mathbf{U}|\mathbf{S}|^{\frac{1}{2}}\mathbf{U}^\top \mathbf{U}_1\mathbf{W}_1^\top \mathbf{W}_2 - \mathbf{U}|\mathbf{S}|^{\frac{1}{2}}\mathbf{W}_1\mathbf{W}_1^\top \mathbf{W}_2 \right]}_{\mathbf{T}_3} \\ &\quad + \underbrace{\left[\mathbf{U}|\mathbf{S}|^{\frac{1}{2}}\mathbf{W}_2 - \mathbf{U}|\mathbf{S}|^{\frac{1}{2}}\mathbf{U}^\top \mathbf{U}_2 \right]}_{\mathbf{T}_4} \\ &\quad + \underbrace{\left[\mathbf{U}|\mathbf{S}|^{\frac{1}{2}}\mathbf{U}^\top \mathbf{U}_2 - \mathbf{U}\mathbf{U}^\top \mathbf{U}_2|\mathbf{S}_2|^{\frac{1}{2}} \right]}_{\mathbf{T}_5} \\ &\quad + \underbrace{\left[\mathbf{U}\mathbf{U}^\top \mathbf{U}_2|\mathbf{S}_2|^{\frac{1}{2}} - \mathbf{U}_2|\mathbf{S}_2|^{\frac{1}{2}} \right]}_{\mathbf{T}_6}. \end{aligned} \tag{6}$$

By Lemma 1, Lemma 2 and Lemma 3, we have that for some constant $c > 0$

$$\begin{aligned} \|\mathbf{T}_2 + \mathbf{T}_3 + \mathbf{T}_4 + \mathbf{T}_5\|_{2 \rightarrow \infty} &= O_p(n^{-1} \gamma^{-1/2}), \\ \|\mathbf{T}_1 + \mathbf{T}_6\|_{2 \rightarrow \infty} &= (1 - \rho)^{1/2} \cdot O_p(n^{-1/2}) + O_p((\log n)^{2c} n^{-1} \gamma^{-1/2}). \end{aligned}$$

Theorem 1 then follows immediately.

Lemma 1. For the term $\mathbf{T}_2, \mathbf{T}_5$ in Eq.(6), we have

$$\|\mathbf{T}_2\|_{2 \rightarrow \infty} = O_p(n^{-1}\gamma^{-1/2}), \quad \|\mathbf{T}_5\|_{2 \rightarrow \infty} = O_p(n^{-1}\gamma^{-1/2}).$$

Proof. For \mathbf{T}_2 we have

$$\begin{aligned} \|\mathbf{T}_2\|_{2 \rightarrow \infty} &\leq \|\mathbf{U}\|_{2 \rightarrow \infty} \cdot \left\| \mathbf{U}^\top \mathbf{U}_1 |\mathbf{S}_1|^{\frac{1}{2}} - |\mathbf{S}|^{\frac{1}{2}} \mathbf{U}^\top \mathbf{U}_1 \right\|_2 \cdot \|\mathbf{W}_1^\top \mathbf{W}_2\|_2 \\ &\leq \|\mathbf{U}\|_{2 \rightarrow \infty} \cdot \left\| \mathbf{U}^\top \mathbf{U}_1 |\mathbf{S}_1|^{\frac{1}{2}} - |\mathbf{S}|^{\frac{1}{2}} \mathbf{U}^\top \mathbf{U}_1 \right\|_2. \end{aligned}$$

For the first part, we have $\|\mathbf{U}\|_{2 \rightarrow \infty} = O_p(n^{-1/2})$. For the second part, we notice that for any $i, j = 1, \dots, d$, the entry ij of it can be written as

$$(\mathbf{U}^\top \mathbf{U}_1 |\mathbf{S}_1|^{\frac{1}{2}} - |\mathbf{S}|^{\frac{1}{2}} \mathbf{U}^\top \mathbf{U}_1)_{i,j} = [\mathbf{U}^\top \mathbf{U}_1]_{i,j} \cdot \left(\sqrt{|\lambda_j(\mathbf{A}_1)|} - \sqrt{|\lambda_i(\mathbf{P})|} \right).$$

So for $i \leq p, j \leq p$,

$$\begin{aligned} (\mathbf{U}^\top \mathbf{U}_1 |\mathbf{S}_1|^{\frac{1}{2}} - |\mathbf{S}|^{\frac{1}{2}} \mathbf{U}^\top \mathbf{U}_1)_{i,j} &= [\mathbf{U}^\top \mathbf{U}_1]_{i,j} \cdot \left(\sqrt{\lambda_j(\mathbf{A}_1)} - \sqrt{\lambda_i(\mathbf{P})} \right) \\ &= [\mathbf{U}^\top \mathbf{U}_1]_{i,j} \cdot (\lambda_j(\mathbf{A}_1) - \lambda_i(\mathbf{P})) \cdot \left(\sqrt{\lambda_j(\mathbf{A}_1)} + \sqrt{\lambda_i(\mathbf{P})} \right)^{-1}. \end{aligned}$$

Similarly, we have for $i > p, j > p$,

$$(\mathbf{U}^\top \mathbf{U}_1 |\mathbf{S}_1|^{\frac{1}{2}} - |\mathbf{S}|^{\frac{1}{2}} \mathbf{U}^\top \mathbf{U}_1)_{i,j} = [\mathbf{U}^\top \mathbf{U}_1]_{i,j} \cdot (\lambda_j(\mathbf{A}_1) - \lambda_i(\mathbf{P})) \cdot \left(-\sqrt{-\lambda_j(\mathbf{A}_1)} - \sqrt{-\lambda_i(\mathbf{P})} \right)^{-1}.$$

For $i > p, j \leq p$,

$$\begin{aligned} (\mathbf{U}^\top \mathbf{U}_1 |\mathbf{S}_1|^{\frac{1}{2}} - |\mathbf{S}|^{\frac{1}{2}} \mathbf{U}^\top \mathbf{U}_1)_{i,j} &= [\mathbf{U}^\top \mathbf{U}_1]_{i,j} \cdot (\lambda_j(\mathbf{A}_1) - \lambda_i(\mathbf{P})) \cdot \left(\sqrt{\lambda_j(\mathbf{A}_1)} + \sqrt{-\lambda_i(\mathbf{P})} \right)^{-1} \\ &\quad + 2 [\mathbf{U}^\top \mathbf{U}_1]_{i,j} \cdot \lambda_i(\mathbf{P}) \cdot \left(\sqrt{\lambda_j(\mathbf{A}_1)} + \sqrt{-\lambda_i(\mathbf{P})} \right)^{-1}. \end{aligned}$$

For $i \leq p, j > p$,

$$\begin{aligned} (\mathbf{U}^\top \mathbf{U}_1 |\mathbf{S}_1|^{\frac{1}{2}} - |\mathbf{S}|^{\frac{1}{2}} \mathbf{U}^\top \mathbf{U}_1)_{i,j} &= [\mathbf{U}^\top \mathbf{U}_1]_{i,j} \cdot (\lambda_j(\mathbf{A}_1) - \lambda_i(\mathbf{P})) \cdot \left(-\sqrt{-\lambda_j(\mathbf{A}_1)} - \sqrt{\lambda_i(\mathbf{P})} \right)^{-1} \\ &\quad - 2 [\mathbf{U}^\top \mathbf{U}_1]_{i,j} \cdot \lambda_i(\mathbf{P}) \cdot \left(\sqrt{-\lambda_j(\mathbf{A}_1)} + \sqrt{\lambda_i(\mathbf{P})} \right)^{-1}. \end{aligned}$$

We define matrices $\mathbf{H}_1, \mathbf{H}_2 \in \mathbb{R}^{d \times d}$ as

$$\begin{aligned} (\mathbf{H}_1)_{i,j} &= \left(\sqrt{|\lambda_j(\mathbf{A}_1)|} + \sqrt{|\lambda_i(\mathbf{P})|} \right)^{-1} \cdot \mathbb{I}(j \leq p) + \left(-\sqrt{|\lambda_j(\mathbf{A}_1)|} - \sqrt{|\lambda_i(\mathbf{P})|} \right)^{-1} \cdot \mathbb{I}(j > p), \\ (\mathbf{H}_2)_{i,j} &= \lambda_i(\mathbf{P}) \cdot \left(\sqrt{|\lambda_j(\mathbf{A}_1)|} + \sqrt{|\lambda_i(\mathbf{P})|} \right)^{-1}. \end{aligned}$$

According to Lemma 4, $\lambda_i(\mathbf{A}_1), \lambda_j(\mathbf{P}) = O_p(n\gamma), \Omega_p(n\gamma)$ for any $i, j \leq d$, it follows that

$$(\mathbf{H}_1)_{i,j} = O_p\left(\frac{1}{\sqrt{n\gamma}}\right), (\mathbf{H}_2)_{i,j} = O_p(\sqrt{n\gamma}).$$

Letting \circ denote the Hadamard matrix product, we arrive at the decomposition

$$\mathbf{U}^\top \mathbf{U}_1 |\mathbf{S}_1|^{\frac{1}{2}} - |\mathbf{S}|^{\frac{1}{2}} \mathbf{U}^\top \mathbf{U}_1 = (\mathbf{U}^\top \mathbf{U}_1 \mathbf{S}_1 - \mathbf{S} \mathbf{U}^\top \mathbf{U}_1) \circ \mathbf{H}_1 + \mathbf{V} \circ \mathbf{H}_2, \quad (7)$$

where

$$\mathbf{V} = \begin{pmatrix} 0 & -2\mathbf{U}_{(+)}^\top \mathbf{U}_{1(-)} \\ 2\mathbf{U}_{(-)}^\top \mathbf{U}_{1(+)} & 0 \end{pmatrix}.$$

The definition of $\mathbf{U}_{(+)}, \mathbf{U}_{(-)}, \mathbf{U}_{1(+)}, \mathbf{U}_{1(-)}$ can be found in Lemma 9, and from the proof of Lemma 9, we know $\|\mathbf{U}_{(+)}^\top \mathbf{U}_{1(-)}\|_F = O_p\left(\frac{1}{n\gamma}\right)$, $\|\mathbf{U}_{(-)}^\top \mathbf{U}_{1(+)}\|_F = O_p\left(\frac{1}{n\gamma}\right)$. So we have $\|\mathbf{V}\|_F = O_p\left(\frac{1}{n\gamma}\right)$. It follows that

$$\|\mathbf{V} \circ \mathbf{H}_2\|_2 \leq d \cdot \|\mathbf{H}_2\|_{\max} \cdot \|\mathbf{V}\|_F = O_p(\sqrt{n\gamma}) \cdot O_p\left(\frac{1}{n\gamma}\right) = O_p\left(\frac{1}{\sqrt{n\gamma}}\right).$$

According to Lemma 5, $\|\mathbf{U}^\top \mathbf{U}_1 \mathbf{S}_1 - \mathbf{S} \mathbf{U}^\top \mathbf{U}_1\|_F = O_p(1)$, thus we have

$$\|(\mathbf{U}^\top \mathbf{U}_1 \mathbf{S}_1 - \mathbf{S} \mathbf{U}^\top \mathbf{U}_1) \circ \mathbf{H}_1\|_2 \leq d \cdot \|\mathbf{H}_1\|_{\max} \cdot \|\mathbf{U}^\top \mathbf{U}_1 \mathbf{S}_1 - \mathbf{S} \mathbf{U}^\top \mathbf{U}_1\|_F = O_p\left(\frac{1}{\sqrt{n\gamma}}\right) \cdot O_p(1) = O_p\left(\frac{1}{\sqrt{n\gamma}}\right).$$

So we bound the spectral norm of $\mathbf{U}^\top \mathbf{U}_1 |\mathbf{S}_1|^{\frac{1}{2}} - |\mathbf{S}|^{\frac{1}{2}} \mathbf{U}^\top \mathbf{U}_1$ as

$$\|\mathbf{U}^\top \mathbf{U}_1 |\mathbf{S}_1|^{\frac{1}{2}} - |\mathbf{S}|^{\frac{1}{2}} \mathbf{U}^\top \mathbf{U}_1\|_2 = O_p\left(\frac{1}{\sqrt{n\gamma}}\right).$$

We finally conclude

$$\|\mathbf{T}_2\|_{2 \rightarrow \infty} \leq O_p\left(\frac{1}{\sqrt{n}}\right) \cdot O_p\left(\frac{1}{\sqrt{n\gamma}}\right) \cdot 1 = O_p\left(\frac{1}{n\sqrt{\gamma}}\right).$$

The proof for $\|\mathbf{T}_5\|_{2 \rightarrow \infty}$ is almost the same. □

Lemma 2. For the term $\mathbf{T}_3, \mathbf{T}_4$ in Eq. (6), we have

$$\|\mathbf{T}_3\|_{2 \rightarrow \infty} = O_p(n^{-1} \gamma^{-1/2}), \quad \|\mathbf{T}_4\|_{2 \rightarrow \infty} = O_p(n^{-1} \gamma^{-1/2}).$$

Proof. For \mathbf{T}_3 we have

$$\begin{aligned} \|\mathbf{T}_3\|_{2 \rightarrow \infty} &\leq \|\mathbf{U}\|_{2 \rightarrow \infty} \cdot \| |\mathbf{S}|^{\frac{1}{2}} \|_2 \cdot \|\mathbf{U}^\top \mathbf{U}_1 - \mathbf{W}_1\|_2 \cdot \|\mathbf{W}_1^\top \mathbf{W}_2\|_2 \\ &\leq \|\mathbf{U}\|_{2 \rightarrow \infty} \cdot \| |\mathbf{S}|^{\frac{1}{2}} \|_2 \cdot \|\mathbf{U}^\top \mathbf{U}_1 - \mathbf{W}_1\|_2. \end{aligned}$$

We notice $\|\mathbf{U}\|_{2 \rightarrow \infty} = O_p(n^{-1/2})$. From Lemma 4, we have $\|\mathbf{P}\|_2 = O_p(n\gamma)$, hence $\|\mathbf{S}^{\frac{1}{2}}\|_2 = (\|\mathbf{S}\|_2)^{\frac{1}{2}} = (\|\mathbf{P}\|_2)^{\frac{1}{2}} = O_p(\sqrt{n\gamma})$. And according to Lemma 9, we have $\|\mathbf{U}^\top \mathbf{U}_1 - \mathbf{W}_1\|_2 = O_p\left(\frac{1}{n\gamma}\right)$. We immediately conclude

$$\|\mathbf{T}_3\|_{2 \rightarrow \infty} = O_p\left(\frac{1}{\sqrt{n}}\right) \cdot O_p(\sqrt{n\gamma}) \cdot O_p\left(\frac{1}{n\gamma}\right) = O_p\left(\frac{1}{n\sqrt{\gamma}}\right).$$

The proof for $\|\mathbf{T}_4\|_{2 \rightarrow \infty}$ is almost the same. \square

Lemma 3. For the term $\mathbf{T}_1, \mathbf{T}_6$ in Eq.(6), we have

$$\|\mathbf{T}_1 + \mathbf{T}_6\|_{2 \rightarrow \infty} = (1 - \rho)^{1/2} \cdot O_p(n^{-1/2}) + O_p((\log n)^{2c} n^{-1} \gamma^{-1/2})$$

for some constant c .

Proof. According to B.2.4 in Rubin-Delanchy et al. (2017),

$$\mathbf{U}_1 |\mathbf{S}_1|^{\frac{1}{2}} = \mathbf{U} |\mathbf{S}|^{\frac{1}{2}} \mathbf{W}_1 + (\mathbf{A}_1 - \mathbf{P}) \mathbf{U} |\mathbf{S}|^{-\frac{1}{2}} \mathbf{W}_1 \mathbf{I}_{p,q} + \mathbf{R}_1,$$

for some (residual) matrix $\mathbf{R}_1 \in \mathbb{R}^{n \times d}$ satisfying $\|\mathbf{R}_1\|_{2 \rightarrow \infty} = O_p\left(\frac{(\log n)^{2c_1}}{n\gamma^{1/2}}\right)$ for some constant $c_1 > 0$. And we notice that $(\mathbf{I} - \mathbf{U}\mathbf{U}^\top)\mathbf{U} = 0$, then

$$\begin{aligned} \mathbf{T}_1 &= (\mathbf{I} - \mathbf{U}\mathbf{U}^\top) \mathbf{U}_1 |\mathbf{S}_1|^{\frac{1}{2}} \mathbf{W}_1^\top \mathbf{W}_2 \\ &= (\mathbf{I} - \mathbf{U}\mathbf{U}^\top) (\mathbf{A}_1 - \mathbf{P}) \mathbf{U} |\mathbf{S}|^{-\frac{1}{2}} \mathbf{W}_1 \mathbf{I}_{p,q} \mathbf{W}_1^\top \mathbf{W}_2 + (\mathbf{I} - \mathbf{U}\mathbf{U}^\top) \mathbf{R}_1 \mathbf{W}_1^\top \mathbf{W}_2 \\ &= (\mathbf{I} - \mathbf{U}\mathbf{U}^\top) (\mathbf{A}_1 - \mathbf{P}) \mathbf{U} |\mathbf{S}|^{-\frac{1}{2}} \mathbf{W}_2 \mathbf{I}_{p,q} + (\mathbf{I} - \mathbf{U}\mathbf{U}^\top) \mathbf{R}_1 \mathbf{W}_1^\top \mathbf{W}_2. \end{aligned}$$

With the similar proof, we have

$$\mathbf{T}_6 = -(\mathbf{I} - \mathbf{U}\mathbf{U}^\top) (\mathbf{A}_2 - \mathbf{P}) \mathbf{U} |\mathbf{S}|^{-\frac{1}{2}} \mathbf{W}_2 \mathbf{I}_{p,q} - (\mathbf{I} - \mathbf{U}\mathbf{U}^\top) \mathbf{R}_2,$$

where \mathbf{R}_2 satisfies $\|\mathbf{R}_2\|_{2 \rightarrow \infty} = O_p\left(\frac{(\log n)^{2c_2}}{n\gamma^{1/2}}\right)$ for some constant $c_2 > 0$. We set $\mathbf{E} = \mathbf{A}_1 - \mathbf{A}_2$.

We therefore have

$$\mathbf{T}_1 + \mathbf{T}_6 = (\mathbf{I} - \mathbf{U}\mathbf{U}^\top) \mathbf{E} \mathbf{U} |\mathbf{S}|^{-\frac{1}{2}} \mathbf{W}_2 \mathbf{I}_{p,q} + \mathbf{R},$$

where we set

$$\mathbf{R} = \mathbf{R}_1 \mathbf{W}_1^\top \mathbf{W}_2 - \mathbf{U}\mathbf{U}^\top \mathbf{R}_1 \mathbf{W}_1^\top \mathbf{W}_2 - \mathbf{R}_2 + \mathbf{U}\mathbf{U}^\top \mathbf{R}_2.$$

We bound the terms of \mathbf{R} one by one. Taking $\mathbf{U}\mathbf{U}^\top \mathbf{R}_1 \mathbf{W}_1^\top \mathbf{W}_2$ as an example, we can bound the $2 \rightarrow \infty$ norm as

$$\begin{aligned} \|\mathbf{U}\mathbf{U}^\top \mathbf{R}_1 \mathbf{W}_1^\top \mathbf{W}_2\|_{2 \rightarrow \infty} &\leq \|\mathbf{U}\mathbf{U}^\top\|_\infty \cdot \|\mathbf{R}_1\|_{2 \rightarrow \infty} \cdot \|\mathbf{W}_1^\top \mathbf{W}_2\|_2 \\ &\leq O_p(1) \cdot O_p\left(\frac{(\log n)^{2c_1}}{n\gamma^{1/2}}\right) \cdot 1 = O_p\left(\frac{(\log n)^{2c_1}}{n\gamma^{1/2}}\right). \end{aligned}$$

Then with the similar analysis, we have $\|\mathbf{R}_1 \mathbf{W}_1^\top \mathbf{W}_2\|_{2 \rightarrow \infty} = O_p\left(\frac{(\log n)^{2c_1}}{n\gamma^{1/2}}\right)$, $\|\mathbf{R}_2\|_{2 \rightarrow \infty} = O_p\left(\frac{(\log n)^{2c_2}}{n\gamma^{1/2}}\right)$, $\|\mathbf{U}\mathbf{U}^\top \mathbf{R}_2\|_{2 \rightarrow \infty} = O_p\left(\frac{(\log n)^{2c_2}}{n\gamma^{1/2}}\right)$. Hence by setting $c = \max\{c_1, c_2\}$, we have

$$\|\mathbf{R}\|_{2 \rightarrow \infty} = O_p\left(\frac{(\log n)^{2c}}{n\gamma^{1/2}}\right).$$

Now we bound the main part of $\mathbf{T}_1 + \mathbf{T}_6$. We first have

$$\|(\mathbf{I} - \mathbf{U}\mathbf{U}^\top) \mathbf{E}\mathbf{U} |\mathbf{S}|^{-\frac{1}{2}} \mathbf{W}_2 \mathbf{I}_{p,q}\|_{2 \rightarrow \infty} \leq \|\mathbf{E}\mathbf{U} |\mathbf{S}|^{-\frac{1}{2}} \mathbf{W}_2 \mathbf{I}_{p,q}\|_{2 \rightarrow \infty} + \|\mathbf{U}\mathbf{U}^\top \mathbf{E}\mathbf{U} |\mathbf{S}|^{-\frac{1}{2}} \mathbf{W}_2 \mathbf{I}_{p,q}\|_{2 \rightarrow \infty}.$$

According to Lemma 6, we have $\|\mathbf{E}\mathbf{U}\|_{2 \rightarrow \infty} = \sqrt{1-\rho} \cdot O_p(\sqrt{\gamma})$, $\|\mathbf{U}^\top \mathbf{E}\mathbf{U}\|_F = \sqrt{1-\rho} \cdot O_p(\sqrt{\gamma})$. We then have

$$\begin{aligned} \|\mathbf{E}\mathbf{U} |\mathbf{S}|^{-\frac{1}{2}} \mathbf{W}_2 \mathbf{I}_{p,q}\|_{2 \rightarrow \infty} &\leq \|\mathbf{E}\mathbf{U}\|_{2 \rightarrow \infty} \cdot \|\mathbf{S}\|_2^{-\frac{1}{2}} \cdot \|\mathbf{W}_2 \mathbf{I}_{p,q}\|_2 \\ &\leq \sqrt{1-\rho} \cdot O_p(\sqrt{\gamma}) \cdot O_p\left(\frac{1}{\sqrt{n\gamma}}\right) \cdot 1 = \sqrt{1-\rho} \cdot O_p\left(\frac{1}{\sqrt{n}}\right), \end{aligned}$$

$$\begin{aligned} \|\mathbf{U}\mathbf{U}^\top \mathbf{E}\mathbf{U} |\mathbf{S}|^{-\frac{1}{2}} \mathbf{W}_2 \mathbf{I}_{p,q}\|_{2 \rightarrow \infty} &\leq \|\mathbf{U}\|_{2 \rightarrow \infty} \cdot \|\mathbf{U}^\top \mathbf{E}\mathbf{U}\|_F \cdot \|\mathbf{S}\|_2^{-\frac{1}{2}} \cdot \|\mathbf{W}_2 \mathbf{I}_{p,q}\|_2 \\ &\leq O_p\left(\frac{1}{\sqrt{n}}\right) \cdot \sqrt{1-\rho} \cdot O_p(\sqrt{\gamma}) \cdot O_p\left(\frac{1}{\sqrt{n\gamma}}\right) \cdot 1 = \sqrt{1-\rho} \cdot O_p\left(\frac{1}{n}\right). \end{aligned}$$

Thus we derive the bound of the main part of $\mathbf{T}_1 + \mathbf{T}_6$ as

$$\|(\mathbf{I} - \mathbf{U}\mathbf{U}^\top) \mathbf{E}\mathbf{U} |\mathbf{S}|^{-\frac{1}{2}} \mathbf{W}_2 \mathbf{I}_{p,q}\|_{2 \rightarrow \infty} = \sqrt{1-\rho} \cdot O_p\left(\frac{1}{\sqrt{n}}\right).$$

We therefore have

$$\|\mathbf{T}_1 + \mathbf{T}_6\|_{2 \rightarrow \infty} = \sqrt{1-\rho} \cdot O_p\left(\frac{1}{\sqrt{n}}\right) + O_p\left(\frac{(\log n)^{2c}}{n\gamma^{1/2}}\right).$$

□

Lemma 4. Let $|\lambda_1(\mathbf{A}_1)| \geq |\lambda_2(\mathbf{A}_1)| \geq \dots$ be the eigenvalues of \mathbf{A}_1 , ordered in decreasing modulus. We then have

$$\lambda_k(\mathbf{A}_1) = \begin{cases} \Omega_p(n\gamma), O_p(n\gamma) & \text{for } k = 1, 2, \dots, d \\ O_p(\sqrt{n\gamma}) & \text{for } k = d + 1, \dots, n \end{cases},$$

The same bounds are true for the eigenvalues of \mathbf{A}_2 . And for the eigenvalues of \mathbf{P} , we have

$$\lambda_k(\mathbf{P}) = \begin{cases} \Omega_p(n\gamma), O_p(n\gamma) & \text{for } k = 1, 2, \dots, d \\ 0 & \text{for } k = d + 1, \dots, n \end{cases}.$$

Proof. Recall the assumption on the maximum expected degree of \mathbf{P} , i.e.,

$$\max_{1 \leq i \leq n} \sum_{j=1}^n \mathbf{P}_{i,j} \geq \max_{1 \leq i \leq n} \sum_{j=1}^n \mathbf{P}_{i,j}(1 - \mathbf{P}_{i,j}) \geq C \ln^4 n.$$

We then have, from Theorem 1 in [Lu and Peng \(2013\)](#) and Weyl's inequality, that

$$\max_{k=1,2,\dots,n} |\lambda_k(\mathbf{A}_1) - \lambda_k(\mathbf{P})| \leq \|\mathbf{A}_1 - \mathbf{P}\|_2 \leq [2 + o(1)] \sqrt{\max_{1 \leq i \leq n} \sum_{j=1}^n \mathbf{P}_{i,j}} = O_p(\sqrt{n\gamma}). \quad (8)$$

Since \mathbf{P} is symmetric and $\text{rank}(\mathbf{P}) = d$, there exists a decomposition $\mathbf{P} = \gamma \mathbf{X} \mathbf{I}_{p,q} \mathbf{X}^\top$, where $\mathbf{X} \in \mathbb{R}^{n \times d}$ and each row of \mathbf{X} corresponds the latent position of each vertex in G_1 , and $\mathbf{I}_{p,q} = \text{diag}(1, \dots, 1, -1, \dots, -1)$ with p ones followed by q minus ones on its diagonal satisfying $p + q = d$. We now consider the eigenvalues of \mathbf{P} . As \mathbf{P} is rank d , we have $\lambda_k(\mathbf{P}) = 0$ for $k > d$. Furthermore, for $k = 1, \dots, d$

$$\lambda_k(\mathbf{P}) = \lambda_k(\gamma \mathbf{X} \mathbf{I}_{p,q} \mathbf{X}^\top) = \gamma \lambda_k(\mathbf{X}^\top \mathbf{X} \mathbf{I}_{p,q}) = n\gamma \cdot \lambda_k\left(\frac{1}{n} \sum_{i=1}^n X_i X_i^\top \mathbf{I}_{p,q}\right),$$

where X_i represents the i th row of \mathbf{X} , i.e., the latent position of i th vertex. Since $\frac{1}{n} \sum_{i=1}^n X_i X_i^\top \mathbf{I}_{p,q}$ converges to a constant matrix, we have

$$\lambda_k(\mathbf{P}) = \begin{cases} \Omega_p(n\gamma), O_p(n\gamma) & \text{for } k = 1, 2, \dots, d \\ 0 & \text{for } k \geq d + 1 \end{cases}.$$

Eq. (8) then implies

$$\lambda_k(\mathbf{A}_1) = \begin{cases} \Omega_p(n\gamma), O_p(n\gamma) & \text{for } k = 1, \dots, d \\ O_p(\sqrt{n\gamma}) & \text{for } k \geq d + 1 \end{cases}.$$

The proof for the eigenvalues of \mathbf{A}_2 is identical. □

Lemma 5. For the term in Eq. (7), we have

$$\|\mathbf{U}^\top \mathbf{U}_1 \mathbf{S}_1 - \mathbf{S} \mathbf{U}^\top \mathbf{U}_1\|_F = O_p(1).$$

Proof. Notice from the block spectral decomposition $\mathbf{A}_1 = \mathbf{U}_1 \mathbf{S}_1 \mathbf{U}_1^\top + \mathbf{U}'_1 \mathbf{S}'_1 \mathbf{U}'_1{}^\top$, we have $\mathbf{A}_1 \mathbf{U}_1 = \mathbf{U}_1 \mathbf{S}_1$. Similarly, we have $\mathbf{P} \mathbf{U} = \mathbf{U} \mathbf{S}$. Then we can split $\mathbf{U}^\top \mathbf{U}_1 \mathbf{S}_1 - \mathbf{S} \mathbf{U}^\top \mathbf{U}_1$ as

$$\begin{aligned} \mathbf{U}^\top \mathbf{U}_1 \mathbf{S}_1 - \mathbf{S} \mathbf{U}^\top \mathbf{U}_1 &= \mathbf{U}^\top \mathbf{A}_1 \mathbf{U}_1 - \mathbf{U}^\top \mathbf{P} \mathbf{U}_1 \\ &= \mathbf{U}^\top (\mathbf{A}_1 - \mathbf{P}) \mathbf{U}_1 \\ &= \mathbf{U}^\top (\mathbf{A}_1 - \mathbf{P}) (\mathbf{I} - \mathbf{U} \mathbf{U}^\top) \mathbf{U}_1 + \mathbf{U}^\top (\mathbf{A}_1 - \mathbf{P}) \mathbf{U} \mathbf{U}^\top \mathbf{U}_1 \end{aligned}$$

And according to Lemma 6 and Lemma 7, we have $\|\mathbf{U}^\top (\mathbf{A}_1 - \mathbf{P})\|_2 = O_p(\sqrt{n\gamma})$, $\|(\mathbf{I} - \mathbf{U} \mathbf{U}^\top) \mathbf{U}_1\|_F = O_p(\frac{1}{\sqrt{n\gamma}})$, $\|\mathbf{U}^\top (\mathbf{A}_1 - \mathbf{P}) \mathbf{U}\|_F = O_p(\sqrt{\gamma})$. We therefore have

$$\begin{aligned} \|\mathbf{U}^\top \mathbf{U}_1 \mathbf{S}_1 - \mathbf{S} \mathbf{U}^\top \mathbf{U}_1\|_F &\leq \|\mathbf{U}^\top (\mathbf{A}_1 - \mathbf{P})\|_2 \cdot \|(\mathbf{I} - \mathbf{U} \mathbf{U}^\top) \mathbf{U}_1\|_F + \|\mathbf{U}^\top (\mathbf{A}_1 - \mathbf{P}) \mathbf{U}\|_F \cdot \|\mathbf{U}^\top \mathbf{U}_1\|_2 \\ &= O_p(\sqrt{n\gamma}) \cdot O_p(\frac{1}{\sqrt{n\gamma}}) + O_p(\sqrt{\gamma}) \cdot 1 = O_p(1). \end{aligned}$$

□

Lemma 6. Let $\mathbf{E} = \mathbf{A}_1 - \mathbf{A}_2$, then

$$\begin{aligned} \|\mathbf{E} \mathbf{U}\|_{2 \rightarrow \infty} &= \sqrt{1 - \rho} \cdot O_p(\sqrt{\gamma}), \quad \|\mathbf{E} \mathbf{U}\|_2 = \sqrt{1 - \rho} \cdot O_p(\sqrt{n\gamma}) \\ \|\mathbf{U}^\top \mathbf{E} \mathbf{U}\|_F &= \sqrt{1 - \rho} \cdot O_p(\sqrt{\gamma}). \end{aligned}$$

For $\mathbf{A}_1 - \mathbf{P}$ and $\mathbf{A}_2 - \mathbf{P}$, we have the same results but without $\sqrt{1 - \rho}$.

Proof. For $\mathbf{U}^\top \mathbf{E} \mathbf{U}$, we note that the ij th element of $\mathbf{U}^\top \mathbf{E} \mathbf{U}$ is of the form

$$(\mathbf{U}^\top \mathbf{E} \mathbf{U})_{i,j} = \sum_{k < l} 2 \mathbf{U}_{k,i} \mathbf{E}_{k,l} \mathbf{U}_{l,j} + \sum_k \mathbf{U}_{k,i} \mathbf{E}_{k,k} \mathbf{U}_{k,j},$$

which is a sum of *independent* mean 0 random variables, and hence by Bernstein's inequality we have

$$(\mathbf{U}^\top \mathbf{E} \mathbf{U})_{i,j} = \sqrt{1 - \rho} \cdot O_p(\sqrt{\gamma}).$$

Since $(\mathbf{U}^\top \mathbf{E} \mathbf{U})$ is a $d \times d$ matrix where d is fixed with n , by the union bound we have

$$\|\mathbf{U}^\top \mathbf{E} \mathbf{U}\|_F = \sqrt{1 - \rho} \cdot O_p(\sqrt{\gamma}).$$

For \mathbf{EU} , we notice

$$\|\mathbf{EU}\|_2 \leq \sqrt{n} \cdot \|\mathbf{EU}\|_{2 \rightarrow \infty} = \sqrt{n} \cdot \max_{1 \leq i \leq n} \|(\mathbf{EU})_i\|_2 = \sqrt{n} \cdot \max_{1 \leq i \leq n} \sqrt{\sum_{j=1}^d (\mathbf{EU})_{i,j}^2},$$

where $(\mathbf{EU})_i$ represents the i th row of (\mathbf{EU}) , and by Bernstein's inequality we have

$$(\mathbf{EU})_{i,j} = \sqrt{1 - \rho} \cdot O_p(\sqrt{\gamma}).$$

We therefore have

$$\|\mathbf{EU}\|_{2 \rightarrow \infty} = \sqrt{1 - \rho} \cdot O_p(\sqrt{\gamma}), \quad \|\mathbf{EU}\|_2 = \sqrt{1 - \rho} \cdot O_p(\sqrt{n\gamma}).$$

For $\mathbf{A}_1 - \mathbf{P}$ and $\mathbf{A}_2 - \mathbf{P}$, the proof is similar. \square

Lemma 7. For terms $\mathbf{U}, \mathbf{U}_1, \mathbf{U}_2$ in the block spectral decompositions of $\mathbf{P}, \mathbf{A}_1, \mathbf{A}_2$, we have

$$\begin{aligned} \|(\mathbf{I} - \mathbf{UU}^\top) \mathbf{U}_1\|_F &= O_p\left(\frac{1}{\sqrt{n\gamma}}\right), \quad \|(\mathbf{I} - \mathbf{UU}^\top) \mathbf{U}_2\|_F = O_p\left(\frac{1}{\sqrt{n\gamma}}\right), \\ \|(\mathbf{U}_1 \mathbf{U}_1^\top - \mathbf{I}) \mathbf{U}_2\|_F &= \sqrt{1 - \rho} \cdot O_p\left(\frac{1}{\sqrt{n\gamma}}\right). \end{aligned}$$

Proof. By applying Theorem 2 in [Yu et al. \(2014\)](#), we have

$$\arg \min_{\mathbf{O} \in \mathbb{O}_d} \|\mathbf{U}_1 - \mathbf{UO}\|_F \leq \frac{2^{3/2} \cdot d^{1/2} \cdot \|\mathbf{A}_1 - \mathbf{P}\|_2}{\lambda_d(\mathbf{P}) - \lambda_{(d+1)}(\mathbf{P})},$$

According to Lemma 4 and Lemma 8, we have

$$\lambda_d(\mathbf{P}) = \Omega_p(n\gamma), \lambda_{(d+1)}(\mathbf{P}) = 0, \|\mathbf{A}_1 - \mathbf{P}\|_2 = O_p(\sqrt{n\gamma}).$$

Thus $\arg \min_{\mathbf{O} \in \mathbb{O}_d} \|\mathbf{U}_1 - \mathbf{UO}\|_F = O_p\left(\frac{1}{\sqrt{n\gamma}}\right)$. We therefore have

$$\begin{aligned} \|(\mathbf{I} - \mathbf{UU}^\top) \mathbf{U}_1\|_F &= \|\mathbf{U}_1 - \mathbf{U}(\mathbf{U}^\top \mathbf{U}_1)\|_F = \arg \min_{\mathbf{T}} \|\mathbf{U}_1 - \mathbf{UT}\|_F \\ &\leq \arg \min_{\mathbf{O} \in \mathbb{O}_d} \|\mathbf{U}_1 - \mathbf{UO}\|_F = O_p\left(\frac{1}{\sqrt{n\gamma}}\right). \end{aligned}$$

The proof for $(\mathbf{I} - \mathbf{UU}^\top) \mathbf{U}_2$ is identical.

From Lemma 8, we have $\|\mathbf{E}\|_2 = \sqrt{1 - \rho} \cdot O_p(\sqrt{n\gamma})$. Then with the similar analysis, we have $\|(\mathbf{U}_1 \mathbf{U}_1^\top - \mathbf{I}) \mathbf{U}_2\|_F = \sqrt{1 - \rho} \cdot O_p\left(\frac{1}{\sqrt{n\gamma}}\right)$. \square

Lemma 8. Let $\mathbf{E} = \mathbf{A}_1 - \mathbf{A}_2$, then

$$\|\mathbf{E}\|_2 = \sqrt{1 - \rho} \cdot O_p(\sqrt{n\gamma}).$$

And similarly, we have

$$\|\mathbf{A}_1 - \mathbf{P}\|_2 = O_p(\sqrt{n\gamma}), \quad \|\mathbf{A}_2 - \mathbf{P}\|_2 = O_p(\sqrt{n\gamma}).$$

Proof. Recall that $\mathbf{E}_{ij} = \mathbf{A}_{1,ij} - \mathbf{A}_{2,ij}$ where $\mathbf{A}_{1,ij}$ and $\mathbf{A}_{2,ij}$ are ρ -correlated Bernoulli random variables. We thus have $\text{Var}[\mathbf{E}_{i,j}] = 2\mathbf{P}_{i,j}(1 - \mathbf{P}_{i,j})(1 - \rho)$. Furthermore, according to our assumption,

$$\max_{1 \leq i \leq n} \sum_{j=1}^n \text{Var}[\mathbf{E}_{i,j}] = 2(1 - \rho) \max_{1 \leq i \leq n} \sum_{j=1}^n \mathbf{P}_{i,j}(1 - \mathbf{P}_{i,j}) \geq 2(1 - \rho) \cdot C \log^4 n.$$

On the other hand, because X_i magnitude does not change with n , $\mathbf{P}_{i,j} = \gamma \cdot X_i \mathbf{I}_{p,q} X_j^\top = O_p(\gamma)$. We therefore have $\max_{1 \leq i \leq n} \sum_{j=1}^n \text{Var}[\mathbf{E}_{i,j}] = (1 - \rho) \cdot O_p(n\gamma)$. Applying Theorem 7 in [Lu and Peng \(2013\)](#) yields the stated claim. The proof for $\|\mathbf{A}_1 - \mathbf{P}\|_2, \|\mathbf{A}_2 - \mathbf{P}\|_2$ is similar. \square

Lemma 9. With proper setting of $\mathbf{W}_1, \mathbf{W}_2$, we can bound $\mathbf{U}^\top \mathbf{U}_1 - \mathbf{W}_1, \mathbf{U}^\top \mathbf{U}_2 - \mathbf{W}_2$ as

$$\|\mathbf{U}^\top \mathbf{U}_1 - \mathbf{W}_1\|_F = O_p\left(\frac{1}{n\gamma}\right), \quad \|\mathbf{U}^\top \mathbf{U}_2 - \mathbf{W}_2\|_F = O_p\left(\frac{1}{n\gamma}\right).$$

Proof. Without loss of generality, we let $\mathbf{U}_1 = [\mathbf{U}_{1(+)} | \mathbf{U}_{1(-)}]$ such that the columns of $\mathbf{U}_{1(+)}$ and $\mathbf{U}_{1(-)}$ consist of orthonormal eigenvectors corresponding to the largest p positive and q negative non-zero eigenvalues of \mathbf{A}_1 , respectively. Similarly, we set $\mathbf{U} = [\mathbf{U}_{(+)} | \mathbf{U}_{(-)}]$. We therefore have

$$\mathbf{U}^\top \mathbf{U}_1 = \begin{pmatrix} \mathbf{U}_{(+)}^\top \mathbf{U}_{1(+)} & \mathbf{U}_{(+)}^\top \mathbf{U}_{1(-)} \\ \mathbf{U}_{(-)}^\top \mathbf{U}_{1(+)} & \mathbf{U}_{(-)}^\top \mathbf{U}_{1(-)} \end{pmatrix} \in \mathbb{R}^{d \times d}.$$

Let $\mathbf{U}_{(+)}^\top \mathbf{U}_{1(+)} = \mathbf{V}_{(+)} \mathbf{\Lambda}_{(+)} \mathbf{V}_{(+)}^\top$ be the singular value decomposition of $\mathbf{U}_{(+)}^\top \mathbf{U}_{1(+)} \in \mathbb{R}^{p \times p}$ and define $\mathbf{W}_{1(+)} = \mathbf{V}_{(+)} \mathbf{V}_{(+)}^\top \in \mathbb{O}_p$. Similarly, define $\mathbf{W}_{1(-)} \in \mathbb{O}_q$ using the singular value decomposition of $\mathbf{U}_{(-)}^\top \mathbf{U}_{1(-)}$ and define \mathbf{W}_1 as the block-diagonal matrix

$$\mathbf{W}_1 = \begin{pmatrix} \mathbf{W}_{1(+)} & 0 \\ 0 & \mathbf{W}_{1(-)} \end{pmatrix} \in \mathbb{O}_d.$$

We now analyze each block of $\mathbf{U}^\top \mathbf{U}_1 - \mathbf{W}_1$. For the first diagonal block,

$$\begin{aligned} \|\mathbf{U}_{(+)}^\top \mathbf{U}_{1(+)} - \mathbf{W}_{1(+)}\|_F^2 &= \text{tr} \left[(\mathbf{U}_{(+)}^\top \mathbf{U}_{1(+)} - \mathbf{W}_{1(+)})(\mathbf{U}_{(+)}^\top \mathbf{U}_{1(+)} - \mathbf{W}_{1(+)})^\top \right] \\ &= \text{tr} (\mathbf{\Lambda}_{(+)}^2 - 2\mathbf{\Lambda}_{(+)} + \mathbf{I}) \\ &= \sum_{i=1}^p (1 - \sigma_i)^2, \end{aligned}$$

where $\sigma_1, \dots, \sigma_p$ are the singular values of $\mathbf{U}_{(+)}^\top \mathbf{U}_{1(+)}$ and $\mathbf{\Lambda}_{(+)} = \text{diag}\{\sigma_1, \dots, \sigma_p\}$. Since $\mathbf{U}_{(+)}$ and $\mathbf{U}_{1(+)}$ both have orthonormal columns, $\|\mathbf{U}_{(+)}^\top \mathbf{U}_{1(+)}\|_2 \leq 1$ and hence, for all $i = 1, 2, \dots, p$,

$$0 \leq 1 - \sigma_i = \frac{1 - \sigma_i^2}{1 + \sigma_i} \leq 1 - \sigma_i^2.$$

We therefore have

$$\sum_{i=1}^p (1 - \sigma_i)^2 \leq \sum_{i=1}^p (1 - \sigma_i^2)^2 \leq \left(\sum_{i=1}^p 1 - \sigma_i^2 \right)^2. \quad (9)$$

Recalling the relationship between the sin- Θ distance and singular values (see e.g., Lemma 1 in [Cai and Zhang \(2018\)](#)), we have

$$\sum_{i=1}^p (1 - \sigma_i^2) \leq \inf_{\mathbf{O} \in \mathbb{O}_p} \|\mathbf{U}_{(+)} - \mathbf{U}_{1(+)} \mathbf{O}\|_F^2.$$

Eq. (9) then implies

$$\|\mathbf{U}_{(+)}^\top \mathbf{U}_{1(+)} - \mathbf{W}_{1(+)}\|_F \leq \inf_{\mathbf{O} \in \mathbb{O}_p} \|\mathbf{U}_{(+)} - \mathbf{U}_{1(+)} \mathbf{O}\|_F^2.$$

By applying Theorem 2 in [Yu et al. \(2014\)](#), we have

$$\inf_{\mathbf{O} \in \mathbb{O}_p} \|\mathbf{U}_{(+)} - \mathbf{U}_{1(+)} \mathbf{O}\|_F \leq \frac{2^{3/2} \cdot d^{1/2} \cdot \|\mathbf{A}_1 - \mathbf{P}\|_2}{\lambda_{(+p)}(\mathbf{P})},$$

where $\lambda_{(+p)}(\mathbf{P})$ is the p -th largest positive eigenvalue of $\mathbf{P} = \mathbb{E}[\mathbf{A}_1]$. According to Lemma 4 and Lemma 8, we have

$$\lambda_{(+p)}(\mathbf{P}) = \Omega_p(n\gamma), \quad \|\mathbf{A}_1 - \mathbf{P}\|_2 = O_p(\sqrt{n\gamma}).$$

We therefore have

$$\inf_{\mathbf{O} \in \mathbb{O}_p} \|\mathbf{U}_{(+)} - \mathbf{U}_{1(+)} \mathbf{O}\|_F = O_p\left(\frac{1}{\sqrt{n\gamma}}\right), \quad \|\mathbf{U}_{(+)}^\top \mathbf{U}_{1(+)} - \mathbf{W}_{1(+)}\|_F = O_p\left(\frac{1}{n\gamma}\right).$$

The same argument also yield $\left\| \mathbf{U}_{(-)}^\top \mathbf{U}_{1(-)} - \mathbf{W}_{1(-)} \right\|_F = O_p((n\gamma)^{-1})$.

We now bound $\mathbf{U}_{(+)}^\top \mathbf{U}_{1(-)}$. Let $u_{(+)}^i$ and $u_{1(-)}^j$ be the i th column of $\mathbf{U}_{(+)}$ and j th column of $\mathbf{U}_{1(-)}$, respectively. The ij -th entry of $\mathbf{U}_{(+)}^\top \mathbf{U}_{1(-)}$ is $(u_{(+)}^i)^\top u_{1(-)}^j$ and hence

$$(u_{(+)}^i)^\top u_{1(-)}^j = \frac{(u_{(+)}^i)^\top (\mathbf{P} - \mathbf{A}_1) u_{1(-)}^j}{\lambda_{(+)}^i(\mathbf{P}) - \lambda_{(-)}^j(\mathbf{A}_1)}.$$

As the positive eigenvalues of \mathbf{P} are separated from the negative eigenvalues of \mathbf{A}_1 , we have, by Lemma 4, $[\lambda_{(+)}^i(\mathbf{P}) - \lambda_{(-)}^j(\mathbf{A}_1)]^{-1} = O_p((n\gamma)^{-1})$. Furthermore, since $(u_{(+)}^i)^\top (\mathbf{P} - \mathbf{A}_1) u_{1(-)}^j$ is the ij -th entry of $\mathbf{U}_{(+)}^\top (\mathbf{P} - \mathbf{A}_1) \mathbf{U}_{1(-)}$, we have

$$\|\mathbf{U}_{(+)}^\top \mathbf{U}_{1(-)}\|_F = O_p\left(\frac{1}{n\gamma}\right) \cdot \|\mathbf{U}_{(+)}^\top (\mathbf{P} - \mathbf{A}_1) \mathbf{U}_{1(-)}\|_F \leq O_p\left(\frac{1}{n\gamma}\right) \cdot \|\mathbf{U}^\top (\mathbf{P} - \mathbf{A}_1) \mathbf{U}_1\|_F.$$

Finally, in Lemma 1, we have proved $\|\mathbf{U}^\top (\mathbf{P} - \mathbf{A}_1) \mathbf{U}_1\|_F = O_p(1)$ and hence

$$\|\mathbf{U}_{(+)}^\top \mathbf{U}_{1(-)}\|_F = O_p\left(\frac{1}{n\gamma}\right).$$

An identical argument also yield $\|\mathbf{U}_{(-)}^\top \mathbf{U}_{1(+)}\|_F = O_p((n\gamma)^{-1})$. Combining the various blocks together, we derive

$$\|\mathbf{U}^\top \mathbf{U}_1 - \mathbf{W}_1\|_F = O_p\left(\frac{1}{n\gamma}\right).$$

The proof for $\|\mathbf{U}^\top \mathbf{U}_2 - \mathbf{W}_2\|_F$ is identical. □

C Additional Results of Data Analysis

Additional results of the simulated and real data are provided in this section. In particular, Appendix C.1 and Appendix C.2 contain additional results of the simulated and real data to illustrate how the choice of the embedding dimension d and the penalty parameter λ affects the performance of our algorithm, respectively; see Figure C1, Figure C2, Figure C3 and Table C1 for the embedding dimension d , and see Table C2, Table C3, Figure C4 and Table C4 for the penalty parameter λ . Figure C5 in Appendix C.3 shows the robustness of our algorithm with different values of the sparsity parameter γ using ρ -SBM setting as an example. Figure C6 and Table C5 in Appendix C.4 illustrate how the reranking step improves the performance of our algorithm for the real data. The comparisons between our algorithm and the embedding followed by Gaussian mixture modeling algorithm of Agterberg et al. (2020) are provided in Appendix C.5. Finally, Figure C10 and Figure C11 in Appendix C.6 show the simulation results when we increase the number of vertices from $n = 300$ (as used in Section 4.1 of the main paper) to $n = 1000$. In particular the performance of our algorithm improves for $n = 1000$ in the ρ -RDPG setting and is stable in the ρ -SBM setting. This is as expected because the latent positions for a ρ -SBM are sampled from a mixture of point masses and hence as n increases the number of points from the same block/classes also increases.

C.1 Results with d changed

	1%	5%	10%	25%	50%	75%	95%	99%
Procrustes ($d = 2$)	0.003	0.013	0.030	0.074	0.196	0.387	0.750	0.870
Procrustes ($d = 3$)	0.002	0.009	0.021	0.071	0.183	0.356	0.792	0.953
Procrustes ($d = 4$)	0.002	0.010	0.021	0.063	0.173	0.361	0.771	0.966
Procrustes ($d = 5$)	0.002	0.009	0.021	0.058	0.164	0.353	0.763	0.950

Table C1: Quantile levels of normalized rank (NR) values for vertex nomination with the Bing entity networks on $n = 1000$ vertices

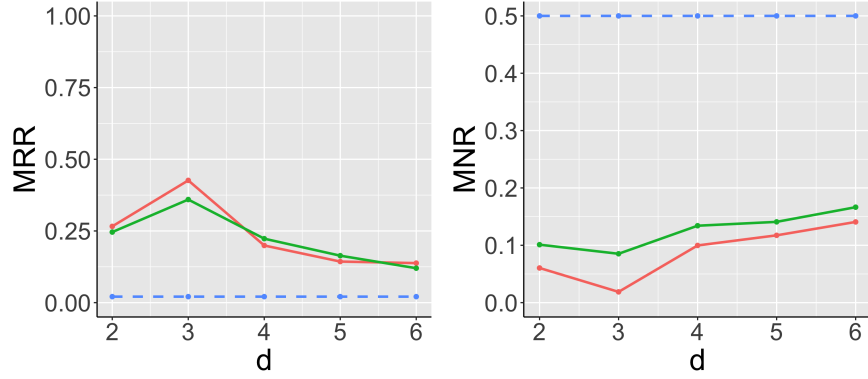


Figure C1: Performance of our algorithm for pairs of ρ -RDPG graphs on $n = 300$ vertices. The mean reciprocal rank (MRR) and mean normalized rank (MNR) are computed based on 500 Monte Carlo replicates. The MRR and MNR are plotted for different values of the embedding parameter d .

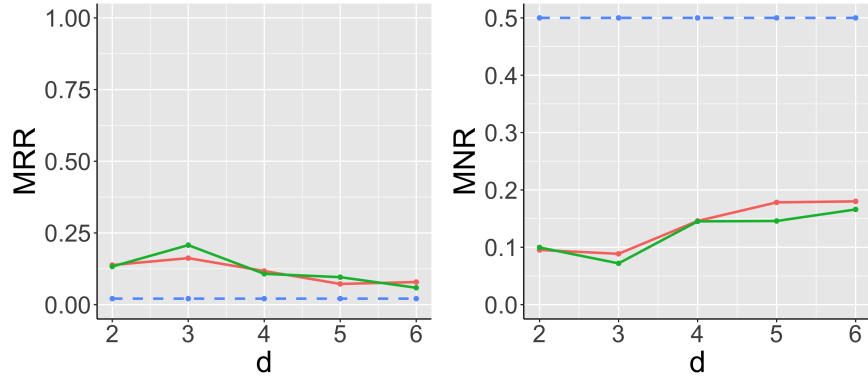


Figure C2: Performance of our algorithm for pairs of ρ -SBM graphs on $n = 300$ vertices. The mean reciprocal rank (MRR) and mean normalized rank (MNR) are computed based on 500 Monte Carlo replicates. The MRR and MNR are plotted for different values of the embedding parameter d .

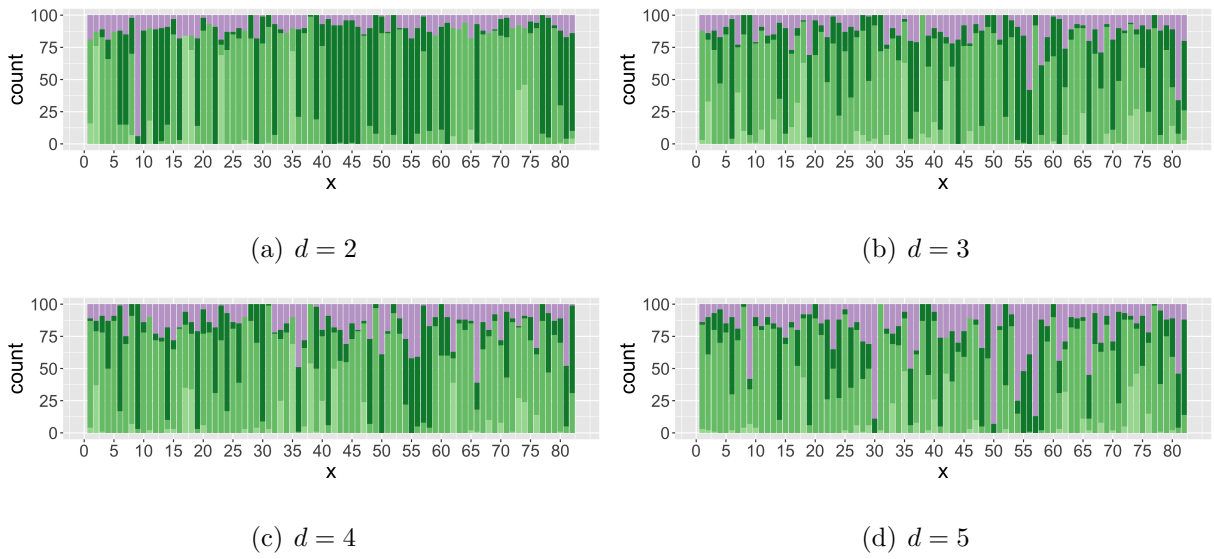


Figure C3: Performance of our algorithm with $d \in \{2, 3, 4, 5\}$ for vertex nomination between the two high-school networks. Here we consider only the subgraphs induced by the 82 shared vertices. The graphs embeddings are aligned via orthogonal Procrustes transformation.

C.2 Results with λ changed

	0.01	0.1	1	10	100
Procrustes	0.494	0.444	0.428	0.432	0.447
set registration	0.427	0.372	0.367	0.370	0.345

Table C2: The mean reciprocal rank (MRR) with different setting of the penalty parameter $\lambda \in \{0.01, 0.1, 1, 10, 100\}$ for pairs of ρ -RDPG graphs on $n = 300$ vertices

	0.01	0.1	1	10	100
Procrustes	0.206	0.182	0.172	0.154	0.159
set registration	0.209	0.208	0.184	0.205	0.168

Table C3: The mean reciprocal rank (MRR) with different setting of the penalty parameter $\lambda \in \{0.01, 0.1, 1, 10, 100\}$ for pairs of ρ -SBM graphs on $n = 300$ vertices

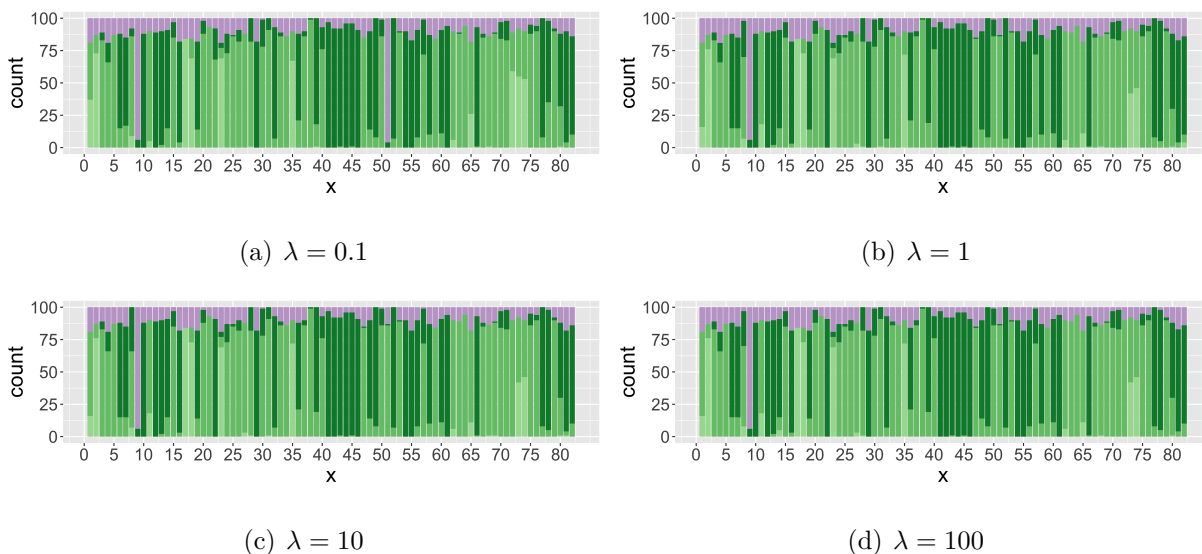


Figure C4: Performance of our algorithm with the penalty parameter $\lambda \in \{0.1, 1, 10, 100\}$ for vertex nomination between the two high-school networks. Here we consider only the subgraphs induced by the 82 shared vertices. The graphs embeddings are aligned via orthogonal Procrustes transformation.

	1%	5%	10%	25%	50%	75%	95%	99%
Procrustes ($\lambda = 0.01$)	0.003	0.012	0.023	0.063	0.180	0.378	0.829	0.904
Procrustes ($\lambda = 0.1$)	0.003	0.013	0.030	0.074	0.196	0.387	0.750	0.870
Procrustes ($\lambda = 1$)	0.003	0.013	0.030	0.074	0.196	0.387	0.750	0.870
Procrustes ($\lambda = 10$)	0.003	0.013	0.030	0.074	0.196	0.387	0.750	0.870
Procrustes ($\lambda = 100$)	0.003	0.013	0.030	0.074	0.196	0.387	0.750	0.870

Table C4: Quantile levels of normalized rank (NR) values for vertex nomination with the Bing entity networks on $n = 1000$ vertices

C.3 Results with γ changed

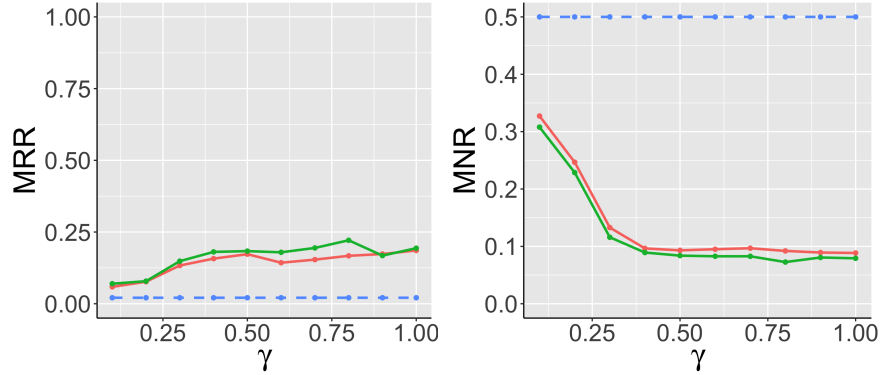


Figure C5: Performance of our algorithm for pairs of ρ -SBM graphs on $n = 300$ vertices. The mean reciprocal rank (MRR) and mean normalized rank (MNR) are computed based on 500 Monte Carlo replicates. The MRR and MNR are plotted for different values of the sparsity parameter $\gamma \in \{0.1, 0.2, 0.3, \dots, 1\}$. We note that different values of $\gamma \geq 0.3$ yield almost identical accuracy.

C.4 Results of reranking step

	1%	5%	10%	25%
Procrustes (100 seeds)	0.002	0.011	0.026	0.073
Procrustes with reranking (100 seeds)	0.001	0.002	0.004	0.027
set registration (100 seeds)	0.002	0.012	0.027	0.073
set registration with reranking (100 seeds)	0.001	0.002	0.004	0.027

Table C5: Quantile levels of normalized rank (NR) values for vertex nomination with and without the reranking step with the Bing entity networks on $n = 1000$ vertices

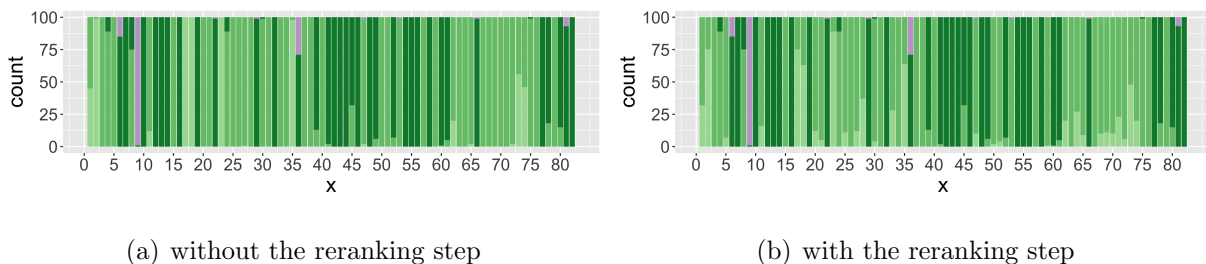


Figure C6: Performance of our algorithm with and without the reranking step for vertex nomination between the two high-school networks. Here we consider only the subgraphs induced by the 82 shared vertices. The graphs embeddings are aligned via orthogonal Procrustes transformation using 10 randomly selected seeds. If a reranking step was done then it was also done using these same seed vertices. The reranking step leads to improved accuracy. In particular, if there was no reranking step then the number of vertices of interest in the first graph for which the corresponding vertex in the second graph has a certain probability of being at the top of the nomination list is 14. This number increases to 29 with the use of the reranking step.

C.5 Comparison with other methods

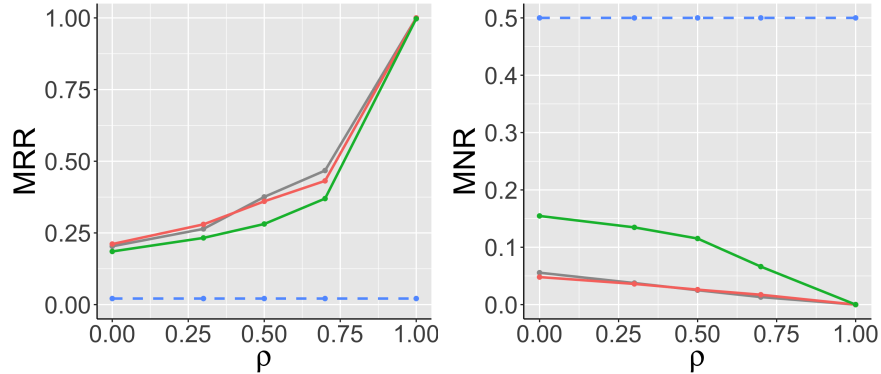


Figure C7: Performance of our algorithm for pairs of ρ -RDPG graphs on $n = 300$ vertices. The mean reciprocal rank (MRR) and mean normalized rank (MNR) are computed based on 500 Monte Carlo replicates. The MRR and MNR are plotted for different values of the sparsity parameter ρ . The grey line corresponds to the method in [Agterberg et al. \(2020\)](#).

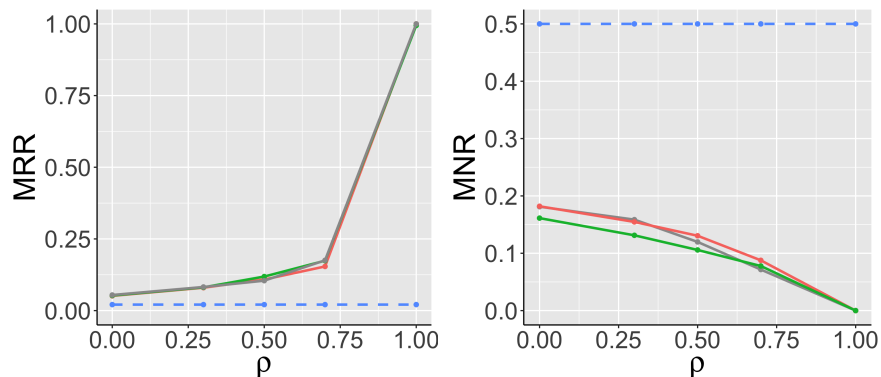


Figure C8: Performance of our algorithm for pairs of ρ -SBM graphs on $n = 300$ vertices. The mean reciprocal rank (MRR) and mean normalized rank (MNR) are computed based on 500 Monte Carlo replicates. The MRR and MNR are plotted for different values of the sparsity parameter ρ . The grey line corresponds to the method in [Agterberg et al. \(2020\)](#).

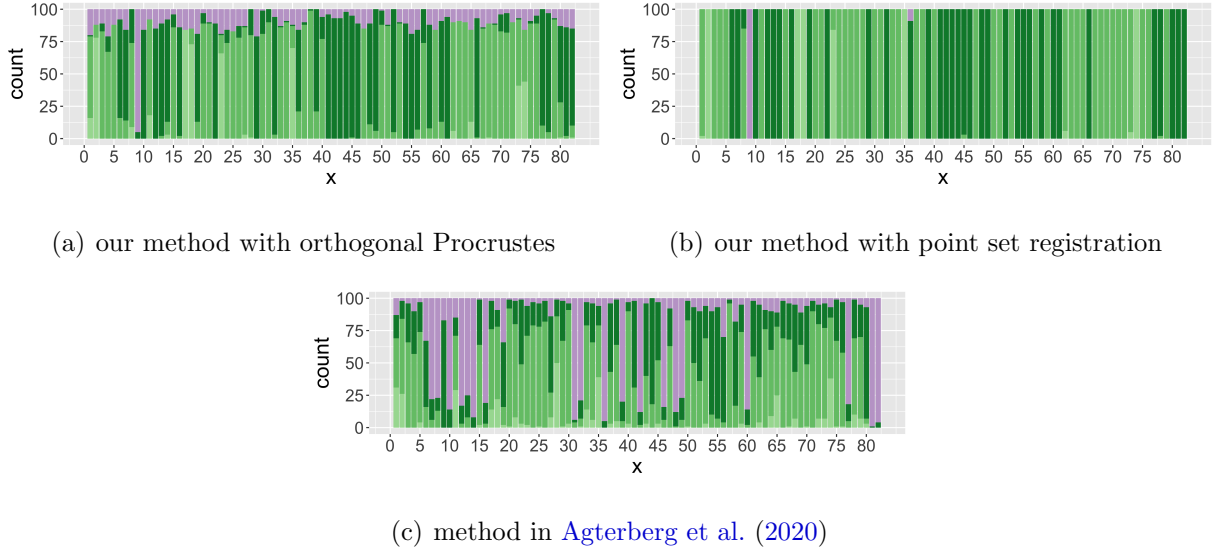


Figure C9: Performance of our algorithm and the method in [Agterberg et al. \(2020\)](#) for vertex nomination between the two high-school networks. Here we consider only the sub-graphs induced by the 82 shared vertices. For our methods, 2 random seeds are also used for the quadratic programming step.

	1%	5%	10%	25%	50%	75%	95%	99%
Procrustes (10 seeds)	0.003	0.013	0.030	0.074	0.196	0.387	0.750	0.870
set registration (no seeds)	0.002	0.013	0.025	0.073	0.196	0.386	0.757	0.876
Agterberg et al. (2020) (10 seeds)	0.003	0.009	0.024	0.076	0.214	0.458	0.744	0.843

Table C6: Quantile levels of normalized rank (NR) values for vertex nomination with the Bing entity networks on $n = 1000$ vertices

C.6 Results of larger n

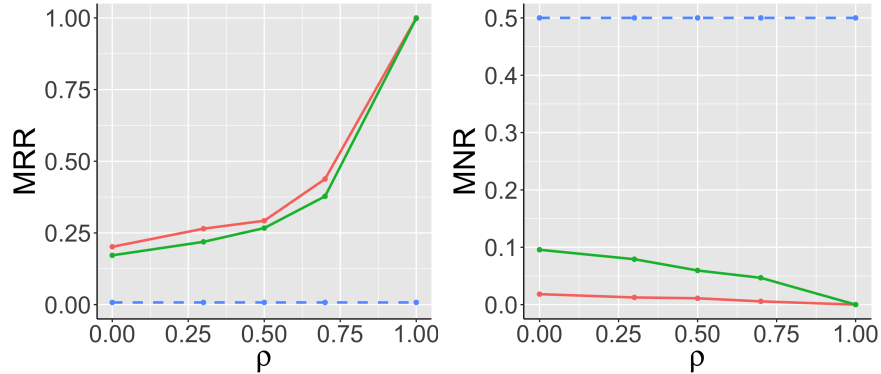


Figure C10: Performance of our algorithm for pairs of ρ -RDPG graphs on $n = 1000$ vertices. The mean reciprocal rank (MRR) and mean normalized rank (MNR) are computed based on 500 Monte Carlo replicates. The MRR and MNR are plotted for different values of the correlation parameter ρ .

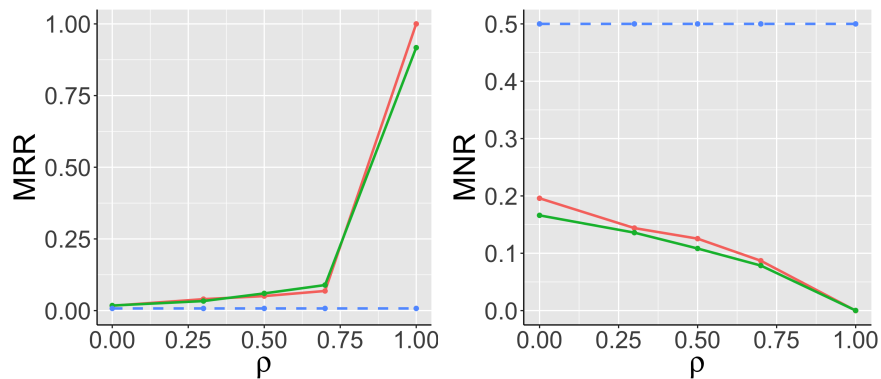


Figure C11: Performance of our algorithm for pairs of ρ -SBM graphs on $n = 1000$ vertices. The mean reciprocal rank (MRR) and mean normalized rank (MNR) are computed based on 500 Monte Carlo replicates. The MRR and MNR are plotted for different values of the correlation parameter ρ .